THE EFFECTS OF DISTRIBUTED LOADS ON INTERNAL FORCES IN THE HAND AND FOREARM

THE EFFECTS OF DISTRIBUTED LOADS ON INTERNAL FORCES IN THE HAND AND FOREARM

By RYAN CHHIBA B.Sc. Kinesiology

A Thesis Submitted to the School of Graduate Studies in Partial Fulfillment of the Requirements for the Degree Master of Science

McMaster University MASTER OF SCIENCE (2023) Hamilton, Ontario

(Kinesiology)

TITLE: The Effects of Distributed Loads on Internal Forces in the Hand and Forearm

AUTHOR: Ryan Chhiba. (McMaster University)

SUPERVISOR: Dr. Peter J. Keir

NUMBER OF PAGES: xvi, 79

ABSTRACT

The hands are essential for our ability to complete tasks. Quantifying the many forces acting on the entire hand is important to improve our understanding of hand function and hand-related musculoskeletal disorders. Biomechanical models of the hand used to compute internal tissue loads typically simplify the applied forces into a single point of force applied at the centre of mass of the distal phalanx. Accounting for the distributed loads across the hands and fingers is a needed step in understanding the loads acting on and inside the body. Therefore, the purpose of this thesis was to use a pressure mapping system to examine the effects of distributed loads on net joint moments and muscle activations in the hands during common tasks. Twenty-three right-handed participants completed a series of finger presses, power grips, and pinch tasks. A pressure mapping system measured pressure on 17 regions of the hand. Three- dimensional hand kinematics was collected using a 72-marker setup. Forces were also measured with a six degrees of freedom force transducer to ensure participants matched specified exertion levels. Pressure distribution, kinematics, and kinetics were used to calculate internal net joint moments at the fingers (distal phalangeal flexion, proximal phalangeal flexion, metacarpal flexion, metacarpal abduction) and muscle activations for 22 forearm and hand muscles using an OpenSim model. External loads were represented in three manners: (1) Centre of Mass Model (COM) distributed the forces over segments that contributed to the force production and placed loads at the centre of mass; (2) Centre of Pressure Model (COP) distributed the forces over segments that contributed to the force production and placed loads at the centre of pressure; (3) Single Point Model (SP) placed a single load at the distal phalanx or the centre of mass of the hand. Results of equivalence tests indicate differences in all net joint moments between COM-SP and COP-SP comparisons. There were no differences between COM and COP. COM and COP moments

during all tasks were larger in digits with a larger percentage of total force compared to SP. Due to the larger moments in those conditions, COM and COP calculated larger muscle activities compared to SP. Both internal net joint moments and muscle activations were most affected by the pressure distribution and hand posture. Overall, these findings indicate that representing external forces using distributed loads provide increased fidelity of forces at the hand and fingers. Distributed loads provide more information on internal loads of the hand and digits, and in turn, quantify individual differences that can lead to injury in occupational settings.

Keywords: Pressure mapping, biomechanical modeling, joint moments, muscle activity

ACKNOWLEDGEMENTS

I am very fortunate to have the help and support from a tremendous group of individuals throughout my Master's. First, I would like to thank my supervisor Dr. Peter Keir, thank you for giving me the opportunity to come McMaster. I am thankful for all your support, and I look forward to working with you over the next few years!

I would like to thank my committee members Dr. Dylan Kobsar, Dr. Aaron Kociolek, and Dr. Jim Lyons. Your expertise and insight at every stage throughout the process helped to significantly improve the quality of my project. I appreciate you all for taking the time to help guide me through this journey and helping me improve as a researcher.

To my lab mates, Daanish Mulla, you have been a mentor and a friend throughout this journey. You were always there to help me and to give me something more to think about. I hope to be half the scientist you are one day. To Nigel Majoni, my brother we started this journey together and my time here would not have been as amazing without you. To Paul Tilley, thank you for starting this project with me, your knowledge and support was essential in completing this thesis and I am happy to have found a friend in you. To Brian Zheng, you were literally the first person I met in Hamilton, and through everything you were there at every step, thank you. To Molly Malette, thank you for all your help, this thesis would not have been collected without you.

To my friends here at McMaster, thank you for your moral and emotional support, I will cherish all the friendship and memories we have made together. A special shoutout to Ally Andrew-Persaud, Sanaa Ahmed, Imaan Ahmed, Sukirat Bhullar, and Mai Wageh. Thank you for supporting me, letting me complain, and encouraging me throughout this degree, I love you!

To my family, thank you Byron Chhiba for driving me back and forth from Hamilton, and supporting me when I ask. Thank you, Prina-ben Mistry, for always being there for me and encouraging me to reach new heights. Thank you, Mom (Jyoti Chhiba) and Dad (Naresh Chhiba), for giving me the privilege of a higher education and letting me pursue my goals. Lastly, I would like to thank the late Mr. Bhikhabhai Chhiba. Dadda, this journey started with you, and I know you are watching and supporting me every day. Love you all!

TABLE OF CONTENTS

LIST OF TABLES

LIST OF FIGURES

LIST OF ABREVIATION

RSI - Repetitive strain injury
CTS - Carpal tunnel syndrome
CMC - Carpometacarpal joint
MCP - Metacarpophalangeal joint
DIP – Distal interphalangeal joint
PIP – Proximal interphalangeal joint
DOF – Degrees of freedom
MVG – Maximum voluntary grip
MFP – Multiple finger press
MFP23 – Multiple finger press with digit 2 and 3
MFP234 – Multiple finger press with digit 2, 3 and 4
MFP2345 – Multiple finger press with digit 2,3,4 and 5
PG – Power grip
MVG – Maximum voluntary grip
PG20 – Power grip at 20% of maximum voluntary grip
PG40 – Power grip at 40% of maximum voluntary grip
COP – Centre of pressure approach
COM – Centre of mass approach
SP – Single point approach
MCP ABD – Metacarpal abduction
MCP FLEX – Metacarpal flexion
PIP FLEX – Proximal interphalangeal flexion
DIP FLEX – Distal interphalangeal flexion
ECRL – Extensor carpi radialis longus
ECRB – Extensor carpi radialis brevis
ECU – Extensor carpi ulnaris
FCR – Flexor carpi radialis
PL – Palmaris longus
FDS 2 – Flexor digitorum superficialis digit 2
FDS 3 –Flexor digitorum superficialis digit 3
FDS 4 – Flexor digitorum superficialis digit 4
FDS 5 – Flexor digitorum superficialis digit 5
FDP 2– Flexor digitorum profundus digit 2
FDP 3– Flexor digitorum profundus digit 3
FDP 4 – Flexor digitorum profundus digit 4
FDP 5 – Flexor digitorum profundus digit 5
EDC 2 – Extensor digitorum digit 2
EDC 3 - Extensor digitorum digit 3
EDC 4 – Extensor digitorum digit 4
EDC 5 – Extensor digitorum digit 5
EDM – Extensor digiti minimi
EIP – Extensor indicis propius
EPL – Extensor pollicis longus
EPB – Extensor pollicis brevis
FPL – Flexor pollicis longus
APL – Abductor pollicis longus
ABP – Abductor pollicis brevis
FPB – Flexor pollicis brevis
OPP – Opponens pollicis
ADPt – Adductor pollicis
ADPo – Adductor pollicis
ADM – Adductor minimus
FDM – Flexor digiti minimi

CHAPTER 1

INTRODUCTION

Our hands allow us to interact with our environment in complex ways. Through these interactions, whether it be during activities of daily living or in the workplace, there is risk in developing hand-related musculoskeletal injuries. In 2021, the Association of Workers' Compensation Boards of Canada reported 48,315 lost time claims due to injury of the upper extremities (*Statistics | AWCBC / ACATC*, 2021). Amongst those claims, 35,408 included injuries to the wrist, hands, and fingers. These injuries impose a burden on workers financially, affect workplace productivity, and task efficiency. Injuries typically result from repeated exposure to forces, and awkward postures over time, rather than from a single, acute event (Keir et al., 2021; Zakaria et al., 2002). Quantifying these risk factors is needed to understand the development of these hand related injuries; however, hand-object interactions that may lead to injury are associated with complex force profiles acting at multiple points on the hand and fingers.

Epidemiological studies identify force as a risk factor to hand injuries yet little work has been done to improve the quantification of hand forces in the field. Most studies use self-reported force exposures or group them into classifications (e.g., light versus heavy). Force is often estimated by gripping force dynamometers or force transducers in similar postures to simulate the task and force load. The estimates do not provide information on the distribution of external forces, and thus cannot provide insight towards the nature of loading and/or injury. Quantifying forces on each part of the hand during hand use will increase our understanding of tissue loading and injury pathomechanics.

Although measuring forces on the hand is difficult, developments in flexible pressure sensors offer a solution. Pressure measurement systems are comprised of arrays of flexible piezoelectric sensors that measure the pressure over a specific area. Pressure mapping provides detailed pressure magnitudes and locations on the palmar surface of the hand. Studies have measured pressure distribution during gripping tasks using rectangular grids on a cylinder (Ergen & Oksuz, 2020; Seo & Armstrong, 2008). Current pressure mapping systems use flexible sensors that may be affixed to gloves, providing a method of collecting region-specific pressures during non-cylindrical gripping tasks and dynamic activities. Pressure mapping systems have been used to quantify gripping pressure limits for robots (Sanford et al., 2014) and determine the role of the index finger during basketball shooting (Hung et al., 2017). A pilot study conducted in our lab used a portable pressure mapping system to quantify the force distribution and centre of pressure during everyday grasping tasks (Chhiba et al., 2022). Using pressure maps will change the representation of external loads in biomechanical hand models, resulting in altered internal loads.

Computational modeling can be used to assess kinematics, calculate joint moments, and estimate internal musculotendon and joint forces (Hicks et al., 2015). Current biomechanical models have a limited representation of the external forces applied to the hands. One such limitation is that contact forces are typically simplified to a single-point force acting at the center of mass (Goislard De Monsabert et al., 2012; Vigouroux et al., 2009). While this assumption allows for simple and computationally efficient models, it is not representative of hand-object interactions. The effects of distributed loads, or multiple points of force application, on internal tissue loads of the hand and forearm has yet to be explored. Considerations of distributed loads should improve our understanding of injury mechanisms during workplace tasks.

We can better characterize external loads using a pressure mapping system and implement a multi-point representation of external loads into biomechanical solutions. This thesis aims to apply pressure mapping technology to determine the multiple points of force application on the hand and evaluate the effect they have on the estimation of internal tissue loading using computational hand models.

CHAPTER 2

LITERATURE REVIEW

2.1 Anatomy of the Hand and Wrist

Twenty-seven bony structures make up the wrist, hand, and fingers. The wrist connects the hands to the upper limb and consists of the proximal carpal row (scaphoid, lunate, triquetrum, pisiform), the distal carpal row (trapezium, trapezoid, capitate, hamate), the radius, and the ulna. There are five carpometacarpal (CMC) joints that connect metacarpals 1-5 to the carpal bones (trapezium, trapezoid, capitate, hamate), respectively (Figure 2.1) (Prendergast & Rauschning, 1995). CMC joints are capable of minimal flexion, extension, adduction, and abduction (Wright, 1935). The metacarpophalangeal (MCP) joints connect the metacarpals to the proximal phalanges (Figure 2.1) and are capable of flexion/extension and abduction/adduction. The proximal interphalangeal (PIP) joints and distal interphalangeal (DIP) joints connect the proximal and distal phalanges of the fingers and are capable of flexion and extension (Wright, 1935) (Figure 2.2).

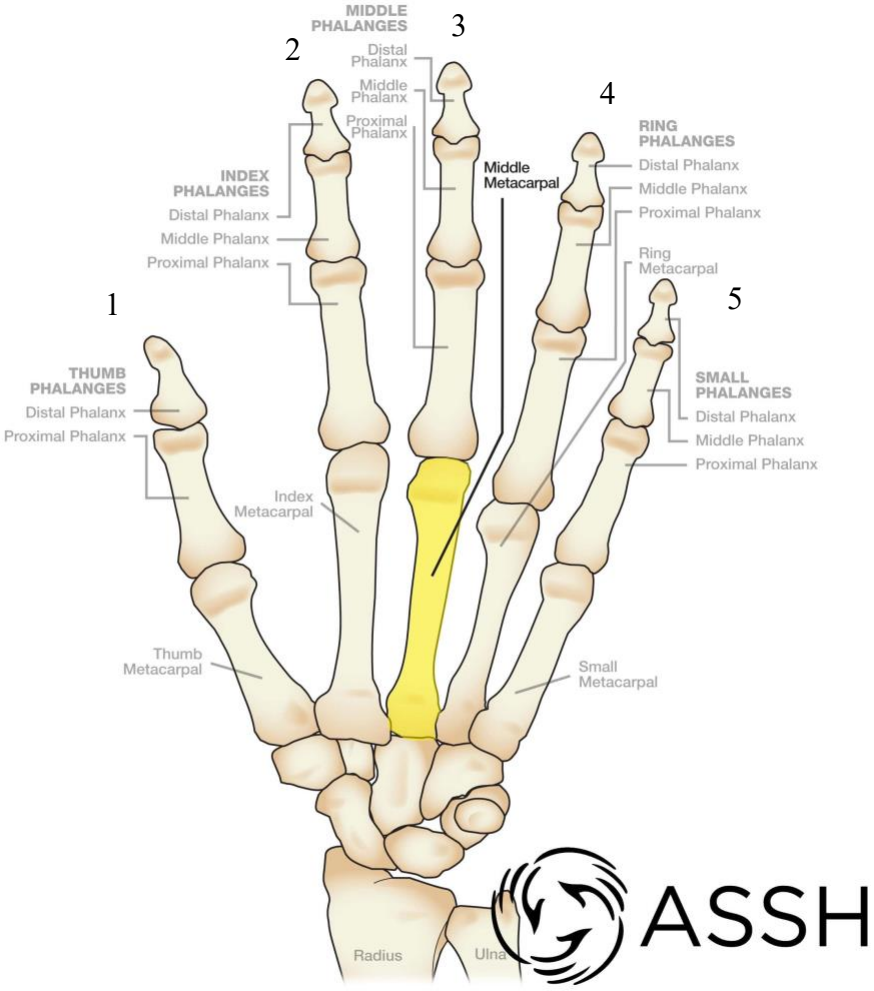

Figure 2.1. The bones of the fingers and wrist (*Hand Surgery Information and Surgeon Database*, 2022)

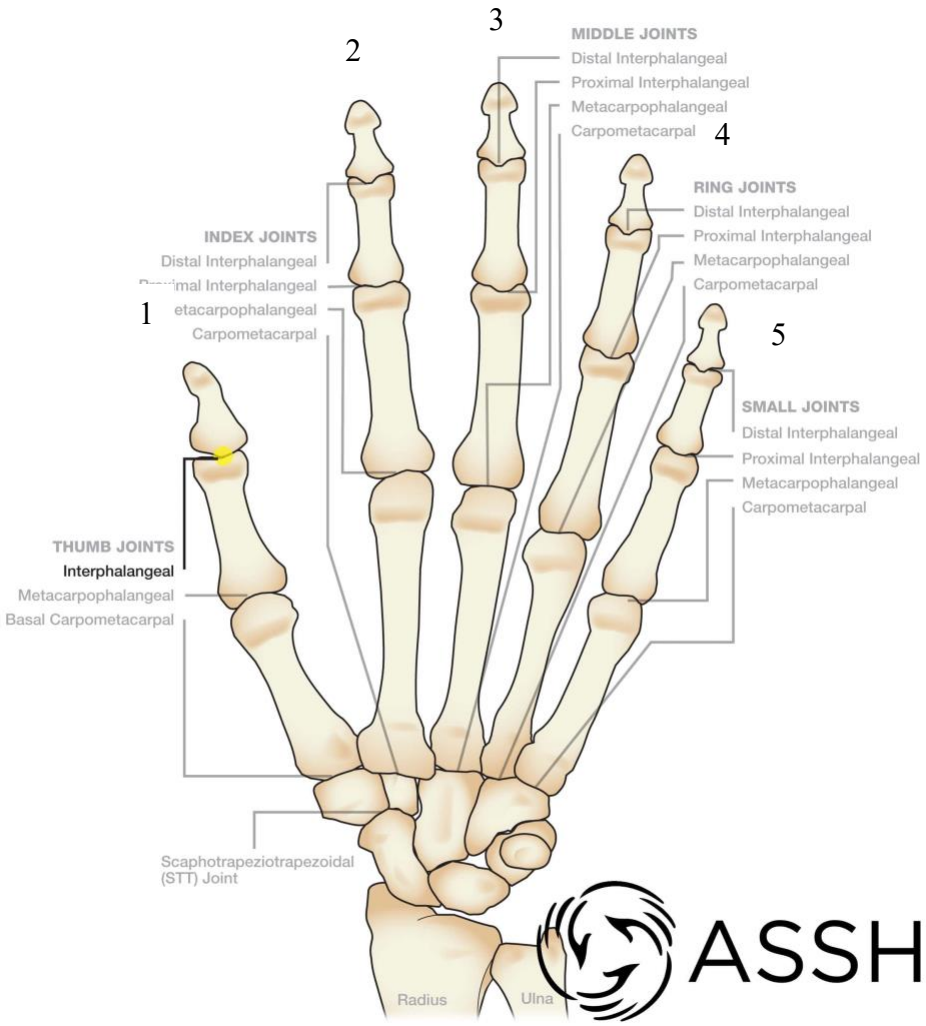

Figure 2.2. Joints of the hands and fingers (*Hand Surgery Information and Surgeon Database*, 2022)

2.2 Muscle Anatomy and Function

Multi-articular muscles span the forearm, hands, and fingers. The muscles that originate in the forearm can be split into an anterior group and posterior group. The anterior group is comprised of flexors (flexor carpi radialis, palmaris longus, flexor carpi ulnaris, flexor digitorum superficialis, flexor digitorum profundus) (Netter, 2011). The posterior group is comprised of extensors of the wrists and fingers. This includes extensor carpi radialis longus, extensor carpi radialis brevis, extensor digitorum, extensor indicis propius, extensor digiti minimi, and extensor

carpi ulnaris (Netter, 2011). Thenar group muscles (flexor pollicis brevis, opponens pollicis, abductor pollicis brevis, adductor pollicis) are intrinsic hand muscles responsible for thumb (digit 1) movements. The hypothenar group muscles (flexor digiti minimi, abductor digiti minimi) are intrinsic hand muscles responsible for little finger (digit 5) movements. Table 2.1 summarizes all the actions of the muscles along with their abbreviations.

Table 2.1: Forearm and hand muscles along with their actions. Abbreviations will be used to refer to each muscle throughout the thesis document.

	Name	Action	Abbreviation
Anterior Group	Flexor Carpi Radialis	Wrist Flexion and Radial Deviation	FCR
	Flexor Carpi Ulnaris	Wrist Flexion and Ulnar Deviation	FCU
	Palmaris Longus	Wrist Flexion	PL
	Flexor Digitorum Superficialis	Wrist Flexion and Finger Flexion	FDS
	Flexor Digitorum Profundus	Wrist Flexion and Finger Flexion	FDP
	Flexor Pollicis Longus	Digit 1 Flexion	FPL
Posterior Group	Extensor Carpi Radialis Longus	Wrist Extension and Radial Deviation	ECRL
	Extensor Carpi Radialis Brevis	Wrist Extension and Radial Deviation	ECRB
	Extensor Carpi Ulnaris	Wrist Extension and Ulnar Deviation	ECU
	Extensor Digitorum	Wrist Extension and Finger Extension	ED
	Extensor Digiti Minimi	Digit 5 Extension	EDM
	Extensor Indicis Propius	Digit 2 Extension	EIP
	Abductor Pollicis Longus	Digit 1 Abduction and Extension	APL
	Extensor Pollicis Longus	Digit 1 Extension	EPL
	Extensor Pollicis Brevis	Digit 1 Extension	EPB
Thenar Muscles	Flexor Pollicis Brevis	Digit 1 Flexion	FPB
	Opponens Pollicis	Digit 1 Opposition	OPP
	Abductor Pollicis Brevis	Digit 1 Abduction	APB
	Adductor Pollicis	Digit 1 Adduction	ADPo & ADPt
Hypothenar Muscles	Flexor Digiti Minimi	Digit 5 Flexion	FDM
	Abductor Digiti Minimi	Digit 5 Abduction	ADM

2.3. Hand Movements and Grasping

Hand movements can be classified as either prehensile (grasping) or non-prehensile (not grasping) (Cutkosky, 1989; Napier, 1956). Prehensile movements are defined as actions that involve grasping an object (Iberall, 1987). Non-prehensile movements are defined as actions that use the fingers or entire hand to push or lift an object. All grasps create an array of forces at different locations across the hands and fingers. Quantifying the multiple forces on the hand during grasps will provide a better understanding of loading patterns and injury mechanisms in the workplace.

2.4 Measuring Forces on the Hand

Pressure mapping systems use tactile pressure sensitive piezoresistive sensors to quantify magnitudes of pressure over grids of sensing elements (Ergen & Oksuz, 2020).The pressure from these devices can be used to calculate load distributions, which is the percent of total pressure applied to a specific area of the hand. The area over which the pressure is applied is known as the contact area. Studies have shown that load distribution and contact area of the hand are affected by grasp type (Ergen & Oksuz, 2020; Mühldorfer-Fodor et al., 2017; Sinsel et al., 2016).

Studies have quantified the contribution of the fingers to the total force during power grips (Austin et al., 2022; Mühldorfer-Fodor et al., 2017; Seo & Armstrong, 2008; Sinsel et al., 2016), and quantified the distributions of loads on the hands and fingers during cylindrical gripping tasks using pressure grids wrapped around cylindrical handles of different diameters. Mühldorfer-Fodor et al. (2017) had participants complete three maximum voluntary grips (MVG) with three handle sizes. Load distribution was split into seven anatomical regions. The average load distribution for the 150 mm cylinder was 11% (thumb), 19% (index finger), 20%

(middle finger), 13% (ring finger), 7% (little finger), 17% (thenar area), and 13% (hypothenar area) (Mühldorfer-Fodor et al., 2017). The 200 mm cylinder had an average load distribution of 18% (thumb), 17% (index finger), 18% (middle finger), 13% (ring finger), 6% (little finger), 20% (thenar area), 9% (hypothenar area) (Mühldorfer-Fodor et al., 2017). There is between participant variability in the contribution of each finger to the load distribution during grasping tasks. Pressure mapping systems can determine pressures and in turn, the forces at each finger, which can help inform the computation of internal loads at the hands and forearm.

Work conducted by Mühldorfer-Fodor et al. (2017), and Sinsel et al. (2016) were limited by the shape of the pressure grid used when collecting data on grasping. As the pressure map was rectangle-shaped, it was only able to be wrapped around cylindrical handles, therefore unable to quantify force distributions during precision grips or other non-power grips. Load distributions were limited to each finger and did not represent each phalange. To provide more insight into forces at the hand, a flexible system with individual sensors for each segment of the hands is needed.

Pressure measurement devices have advanced to become highly mobile. In recent studies, the use of pressure mapping gloves has gained popularity. The system consists of a glove affixed with piezoresistive sensors (Hung et al., 2017; Mastalerz et al., 2009; Sanford et al., 2014; Sinsel et al., 2016). The TekScan Grip system (TekScan Inc, Boston, MA, USA) is a pressure mapping system that consists of 17 sensing regions on the palmar surface of the hand that corresponds to the anatomy of the fingers and hand. There are 2 sensing regions on the thumb, 3 on each finger, corresponding to the distal, middle, and proximal phalanges, and 3 on the palm (metacarpophalangeal heads, thenar, and hypothenar regions). Sanford et al. (2014) used the TekScan Grip system to collect pressure mapping data of 20 participants to identify gripping

strategies when pushing and pulling a door. They reported the maximum detected pressure for each sensor and distinguished three gripping patterns – “palm”, “fingertips” or “both” – based on the primary interaction areas (areas with the highest detected pressure). Ergen and colleagues (2020) used the same system to quantify the multiple points of pressure and contact area during four common gripping tasks (standard grip, pinch grip, lateral grip, and tripod grip). The contact area was defined as the area of the sensing regions activated (square centimetres). The pressure and contact area differed for all tasks. The standard grip had the largest pressure over the middle finger while the highest contact area was over the distal MCP heads. For the lateral and pinch grip, the pressure was highest at the index finger while the highest contact area was at the thumb. During the tripod grip (also referred to as the three-finger chuck), they reported the highest pressure and contact area at the distal thumb. The high variability in this study reiterates the need to assess the impact of the forces of the hand on internal tissue loading. Both of these studies (Ergen & Oksuz, 2020; Sanford et al., 2014), quantified the pressure of the tasks but did not identify the centre of pressure of each sensor as points of force application may not be acting at the centre of mass. They also did not control for exertion level, therefore making it difficult to quantify muscle contributions.

An independent study was recently conducted in our lab using the TekScan Grip system. Force distribution and centre of pressure for each sensor was quantified during common gripping tasks (Chhiba et al., 2022). Nine static tasks were chosen: (i) medium wrap, (ii) lateral pinch, (iii) three-finger chuck, (iv) power sphere grip, (v) index finger extension, (vi) table lean, (vii) lateral pinch, (viii) standard pinch grip, and (ix) standard power grip. The pressure and centre of pressure were collected for each sensor. Results showed that there was variability in the force distribution and centre of pressure during gripping tasks within and between participants.

Between participant variability was higher than within participant variability but, was not further evaluated as force and exertion levels were not controlled.

The variability seen in previous work emphasizes that there are differences in how tasks are performed between participants and by an individual. As a result, the location of the distributed external loads varies across each segment of the hand. An assumption that the loads act at the centre of mass may not be representative of the multiple points of loading. The effects of these load distributions and variability on internal tissue loading is not known.

The pressure mapping gloves are not without their limitations. Personal experience and the literature have noted that the glove the sensors have been affixed to hinders the ability to manipulate objects (Ergen & Oksuz, 2020), where finger range of motion may be impeded by the thickness of the glove. The difference in friction due to the sensors and glove compared to the skin may also affect the forces generated by the hands and require a higher force to grip objects (Lemerle et al., 2008). The bulky nature of the system presents a challenge when trying to collect multiple measures (kinematics and electromyography) of the forearm and hand. The glove and other apparatus cover the hands and part of the forearm, which may hinder the other measurements needed as inputs for the biomechanical model. It should be noted that sensors are only able to collect pressure data directly in one plane, so any off-axis forces may not be adequately quantified. Even with limitations, pressure mapping gloves present a method of collecting data within the workplace to estimate internal joint loading.

2.5 Biomechanical Modelling of the Hand

Many biomechanical models of the hand have been developed to assess the effect of external forces on internal loading (Holzbaur et al., 2005; McFarland et al., 2023; Mirakhorlo et

al., 2018; Vigouroux et al., 2009). They have continued to evaluate hand and finger forces in a variety of conditions. A dynamic model of the index finger developed by Brook et al. (1995), evaluated the tendon forces and muscle activity during a pinching task. A 1 Newton (N) pinch force was placed at the centre of the distal phalanx in the vertical direction (Brook et al., 1995). Vigouroux et al. (2009) compared the results of two different thumb models when evaluating tendon tension. Kinematic data was collected on 6 participants completing pulp and pinch grips. A 1 N fingertip force was simulated at the midpoint of the distal phalanx in 45-degree increments in the medial, lateral, palmar, and dorsal directions. Both models were able to predict muscle activation for five out of the nine muscles that were modelled. Previous work in our lab improved the co-contraction estimates of the index finger using electromyographical constraints (MacIntosh & Keir, 2017). Muscle activations were assessed during different postures of index finger pressing. This model improved our anatomical fidelity of the finger by better predicting muscle co-contraction but does not account for loading of the other fingers (thumb, middle, ring, and little). Mirakhorlo et al. (2018) built a hand model in OpenSim, an open-source musculoskeletal modelling software. They simulated a 2 N to 10 N pinch force located 22 mm distally from the DIP of the index finger. Their model computed muscle forces (flexor digitorum superficialis and flexor digitorum profundus) and moments (MCP and wrist flexion moments) comparable to experimentally collected data. The predicted tendon forces (25 N) were comparable to results from an in surgical experimental study (22 N) (Kursa et al., 2005). Most recently, McFarland et al. (2023) evaluated their biomechanical model of the hand and wrist by predicting thumb muscle force during a lateral pinch through static optimization. They simulated pinch forces from 0 N to 60 N (in 10 N increments) placed at the tip of the distal phalanx of the thumb. Experimentally derived forces under similar conditions were reported to be 51.9 ± 20.9 N

(Valero-Cuevas et al., 2003) and simulations resulted in 66.3 ± 2.3 N. The models work well to predict muscle forces and improve their anatomical fidelity yet continue to represent a single force acting at the midpoint of the finger or thumb.

While all the models produced results comparable to the literature, all external forces applied to the fingers were single points acting at the middle of the segment or the tip of the distal phalanx. The literature focuses on varying the magnitude of forces but not the location. This limitation can be overcome by using a pressure mapping system to provide the appropriate magnitude of the force (force distribution) and the location of forces (at the centre of pressure). Sinsel et al. (2016) used a pressure mapping glove to quantify the load distribution and centre of pressure during cylindrical gripping tasks to be used as inputs for inverse dynamics. Pressure mapping systems offer the ability provide more information on how much and where the forces are acting. The effects of single finger forces on joint loading have been reported (MacIntosh & Keir, 2017; McFarland et al., 2023; Mirakhorlo et al., 2018; Valero-Cuevas et al., 2003; Vigouroux et al., 2009) yet, there has not been work on the effects of multiple forces acting across the entirety of the hand. Adding in multiple points of force application at their centre of pressure may provide a more realistic representation of loading at the fingers and wrist and therefore increase the accuracy of internal joint loading predictions.

2.6 Summary

The hands can complete a variety of grasping tasks that require the exertion of forces across the palmar surface of the hand. Quantifying the magnitude and location of forces will play an important role in predicting internal joint loading and our understanding of injury pathomechanics. Pressure mapping measurement system can be used to better describe the

distributed forces acting across multiple points on the hands. Previous literature has utilized models that represent loads as a single point force at the centre of mass of the segment. While this representation of external loading preserves the computational efficiency of the model, it does not account for the multiple points of force application and the fact that forces may be acting at a different part of the segment depending on the task. When considering the cumulative effect of multiple points of force application not at the centre of mass, there will be a difference in the moment arms and therefore internal net joint moments. The effect of multiple points of force application on predictive joint loading calculations has yet to be explored. The opportunity to use pressure mapping systems to identify multiple points of force and quantify center of pressure as inputs for biomechanical models will allow us to better quantify forces at the hand. This new model will increase the computational fidelity of musculoskeletal models of the hands and fingers and will help guide prevention and intervention techniques in the workplace.

CHAPTER 3

RESEARCH OBJECTIVES AND HYPOTHESES

3.1 Research Objective

The overall goal of this thesis was to explore the effects of multi-point force application inputs on the computation of internal joint loads of the hands using biomechanical models. This thesis has two research questions:

1. How are net joint moments of the wrist and fingers affected by the changes in force location and distributions of external forces compared to single point of force application?
2. How are forearm and fingers muscle activations affected by the changes in force location and distributions of external forces compared to single point of force application?

3.2. Hypotheses

The following hypotheses can be generated from the objectives.

1) Using centre of mass (COM) and centre of pressure (COP) representations of force application will result in lower metacarpophalangeal joint abduction (MCP ABD), metacarpophalangeal joint flexion (MCP FLEX), proximal interphalangeal joint flexion (PIP FLEX), and distal interphalangeal joint flexion (DIP FLEX) moments when compared to the single point (SP) model. As the force and moment arms should be higher in the SP model, it is expected to compute higher net joint moments. The COP is expected to have larger moments due to the larger moment arms than COM. The power grip and pinch tasks are expected to have larger moments due to the larger overall forces compared to the single and multi-finger presses.

2) Inputting forces using the centre of mass (COM) and centre of pressure (COP) models will result in less flexor/extensor muscle activations compared to the single point (SP) model. Similar to above, the higher forces in the SP model will result in larger muscle activations. The larger moment arms in COP will lead to larger activations when compared to COM. The power grip and pinch tasks will have larger forces resulting in larger activations when compared to the single finger and multi finger presses.

CHAPTER 4

METHODS AND ANALYSIS

4.1 Participants

A total of 23 healthy right-hand dominant participants aged 19-30 were recruited (10 females, 13 males). Exclusion criteria consisted of participants who experienced any upper extremity injuries in the past 6 months. Body height, body weight, hand width, digit lengths, index finger middle phalanx circumference, and hand breadth were recorded for each participant. Ethics clearance was obtained from the McMaster Research Ethics Board (MREB #: 5880).

4.2 Instrumentation

A hand pressure mapping system (Tekscan Grip System, TekScan Inc, Boston, MA) was used to collect pressure and determine the local centre of pressure in each region of the hand. The 17 sensing regions were affixed to a golf glove (Stratus Tech Glove, TaylorMade, Carlsbad, CA) (Figure 4.1A), with each region corresponding to specific areas on the palmar surface of the hand (Figure 4.1B). Five different glove sizes were provided for participants to wear: Men's Medium, Large, Extra-Large, and Women's Small, Medium to ensure the sensors were placed over the appropriate anatomical regions. Before each collection, the TekScan sensors were calibrated using a point calibration. A 10 N force was applied over the sensels within a sensor region using a MARK-10 force transducer with a rubber attachment (Mark-10 Corporation, Copiague, NY). This process was repeated on each of the 17 sensing regions on the TekScan Grip System.

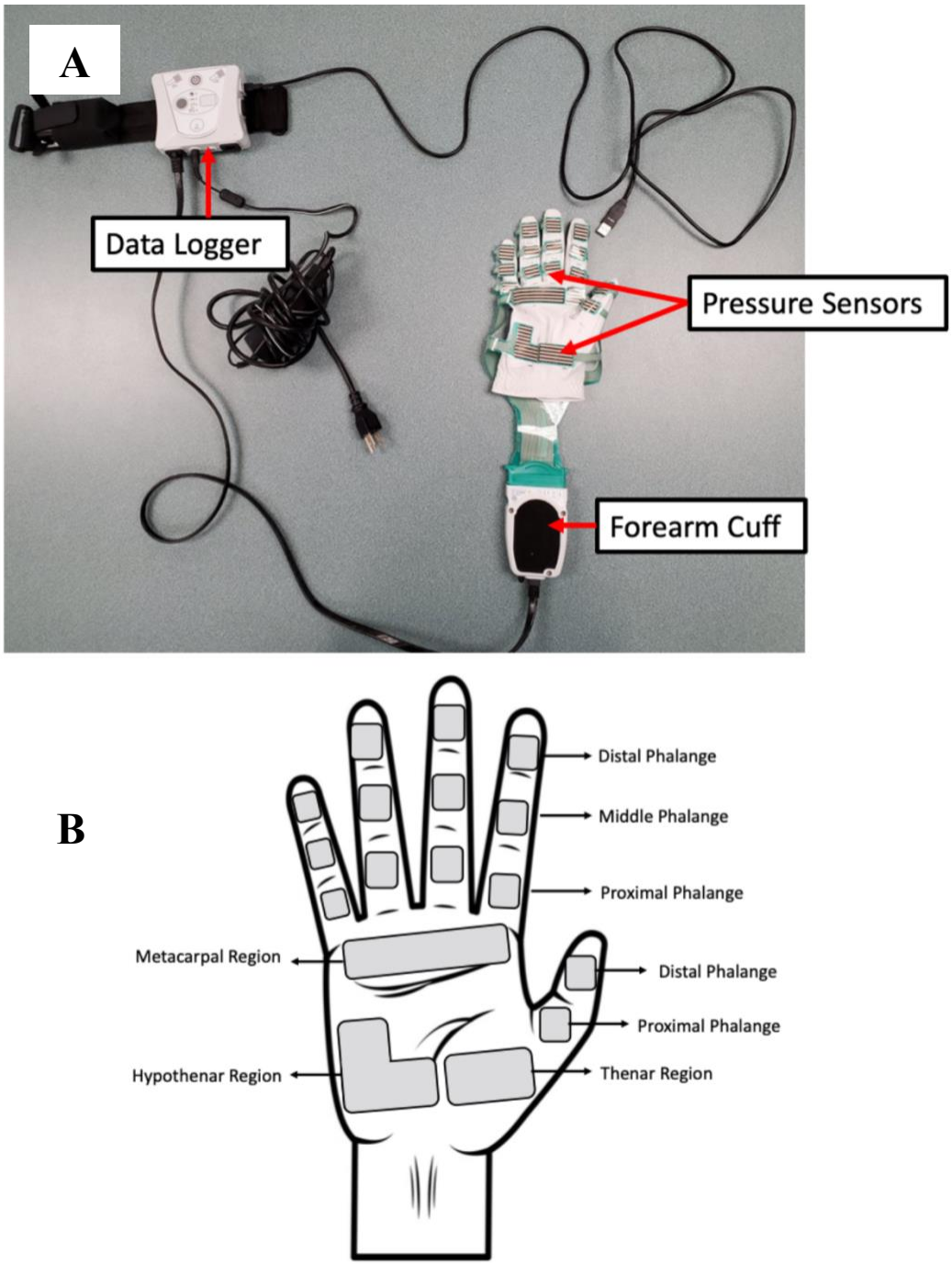

Figure 4.1. A) Tekscan grip system affixed to the TaylorMade glove. Anatomical locations of Tekscan Grip system sensors consisting of two regions of the thumb (proximal and distal phalanges), three regions on each of fingers 2-5 (proximal, middle, and distal phalanges), and three regions on the palm (heads of 2nd-5th metacarpals, thenar palm, hypothenar palm). The sensors are attached to the cuff and the TekScan system datalogger. B) Placement of the 17 TekScan sensors across the palmar surface of the right hand

A force transducer (MC3-500, AMTI, Watertown MA, USA) collected forces at 1000 Hz in the Fx, Fy, and Fz directions. A digital hand grip dynamometer collecting at 1000 Hz measured grip force during the power gripping tasks (MIE, Leeds, United Kingdom).

A three-dimensional passive motion-based capture system comprised of 11 Raptor-4 cameras (MotionAnalysis Corporation, Santa Rosa CA, USA) was used to measure upper arm kinematics during the tasks. Marker data was sampled at 50 Hz with a total of 72 2-mm reflective markers placed on the participant. Markers were placed on anatomical landmarks including the lateral and medial epicondyles of the humerus, the olecranon, the middle of the humerus, the radial styloid, and the ulnar styloid. Tracking marker clusters were placed at the middle of the forearm and the dorsal surface of each digit's metacarpal, proximal phalanx, middle phalanx, and distal phalanx. Joint markers were placed on the dorsal surface overlying each MCP and each IP joint (PIP and DIP) (Figure 4.2). Marker placement was based on recommendations from the International Society of Biomechanics (Wu et al., 2005).

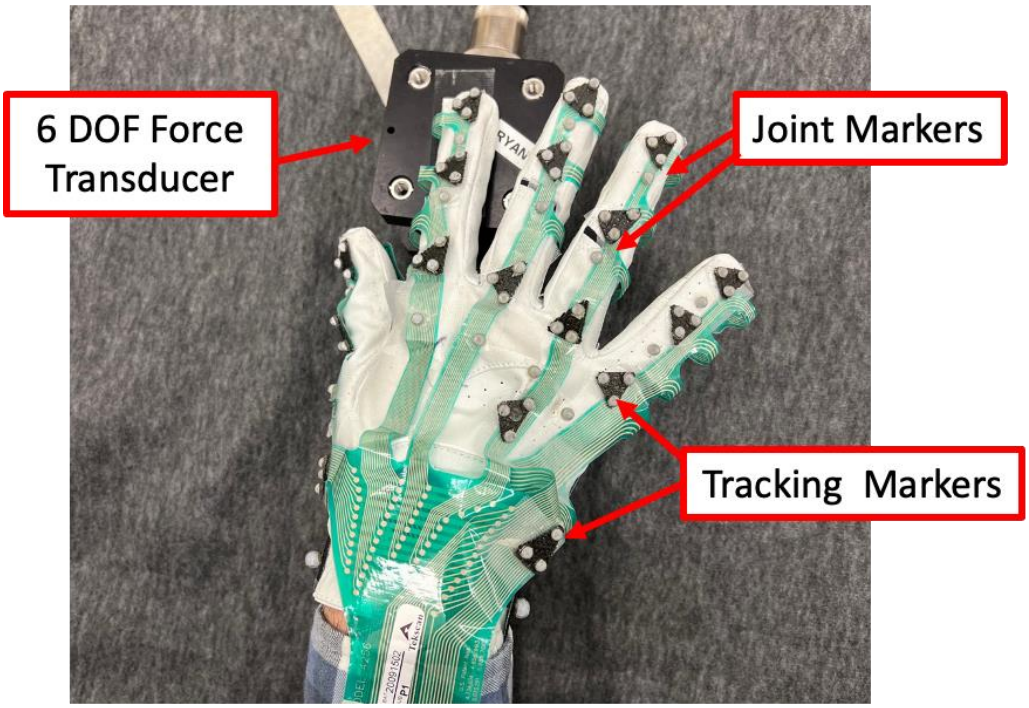

Figure 4.2. Marker placement on participants and glove. Markers were placed at the lateral and medial epicondyles of the humerus, the olecranon, the middle of the humerus, the radial styloid, and the ulnar styloid. Tracking marker clusters were placed at the middle of the forearm, each metacarpal, each proximal phalange, middle phalange, and each distal phalange. Joint markers were placed at each MCP joint, and each IP joint (PIP and DIP).

4.3 Experimental Setup and Protocol

First, the participant provided written informed consent. Preliminary anthropometric measurements were taken of body height, body weight, hand width, hand length, hand breadth, each finger length, and index finger circumference. Next, participants were fitted with a golf glove with the affixed TekScan sensors which was then equipped with reflective markers. Once the markers were placed, the participant was seated at the table (See Appendix A, Figure 1). The table height was adjusted to ensure the participant was sitting upright and their elbow was flexed to 90°. The force transducer was then placed under their hand at a comfortable distance away from them, to maintain 90° of elbow flexion, no shoulder flexion, and a neutral wrist posture.

Each participant completed two maximum voluntary grips (MVG) with two minutes of rest between repetitions. The average of the two trials was used as their MVG force. Ten static tasks were performed by each participant. Tasks consisted of multiple fingers pressing, power gripping, pinching and single finger pressing exertions as outlined in Figures 4.3, 4.4, 4.5, and 4.6. Participants were instructed to use their right hand to complete the tasks while maintaining the specified force. A computer monitor displayed the target force, that the participant was asked to match. Before each task, participants were given the chance to perform a practice trial for familiarization. Each trial would begin with the visual force feedback to give the participant time to ramp up the desired target force. Once the force target was met, force, kinematics and pressure data were collected for 10 seconds. Tasks were completed in a block randomized order and each participant completed each task a total of three (3) times with 30 seconds of rest between each trial and one minute between tasks. This gave enough time to explain each new task to the participant and provided an adequate amount of rest.

Figure 4.3. Multi- Finger Press (MFP). Participants pressed down on the force transducer with the specified digits and at the specified force. Trials were accepted if participants held the press within a range of +/- 2 N of the specified force.

Figure 4.4. Power Grip (PG). Using the hand grip dynamometer, participants held the handle with their index finger on the white tape. They were instructed to grip the dynamometer with all their fingers at the required %MVG (40% or 20%). Participants must hold the grip within a range of +/- 2% of their averaged power grip MVG force.

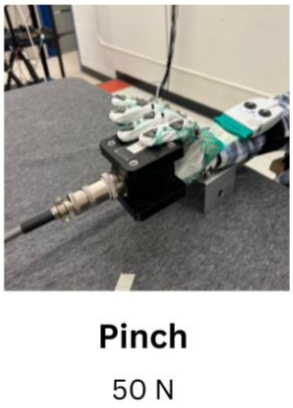

Figure 4.5. Pinch. Participants held the force transducer with the distal tips of digit 2,3,4 and 5 at the top and digit 1 at the bottom. They were instructed to squeeze to the specified force.

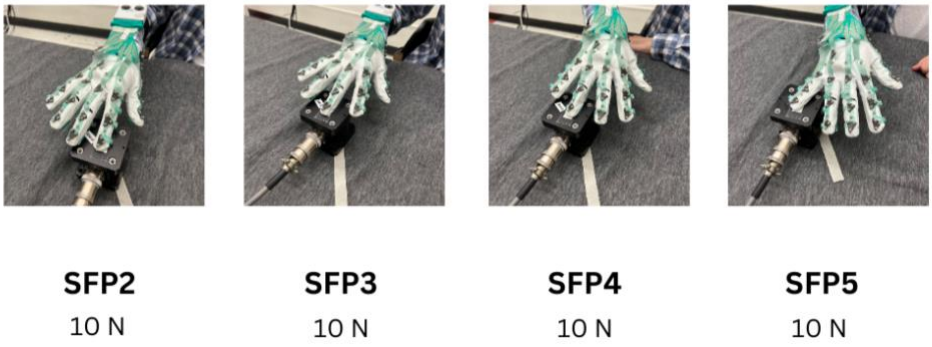

Figure 4.6. Single Finger Press (SFP). Participants pressed down on the force transducer with the specified digit and at the specified force. Trials were accepted if participants held the press within a range of +/- 1 N of the specified force.

4.4 Biomechanical Hand Model

This thesis used the ARMS Hand and Wrist OpenSim model developed by McFarland et al. (2023). It is the most recent and complete biomechanical model of the wrist, hand, and fingers currently available. As an extension of previous work (Barry et al., 2018; Nichols et al., 2017), this model includes 22 rigid bodies, with mass and inertial properties for the individual bone segments of the phalanges, metacarpals, carpals, and forearm bones. It also has 23 independent degrees of freedom (DOF) including a flexion/extension DOF at each IP joint of all five digits (9 DOFs), flexion/extension and abduction/adduction DOFs at the MCP joint of digit 1 to 4 (8 DOFs), flexion/extension DOF at the MCP joint of the thumb (digit 1) (1 DOF), flexion/extension and abduction/adduction DOF at the CMC thumb joint (2 DOFs), a coupled flexion DOF for the CMC joints of the ring and little finger (1 DOF), and flexion/extension and radial/ulnar deviation DOF at the wrist (2 DOFs) (McFarland et al., 2023). This model also includes passive joint properties for all flexion/extension DOF of the phalanges and thumb, for CMC abduction/adduction of the thumb, and wrist flexion and deviation DOF. Forty-three Hill-type muscle-tendon actuators representing the intrinsic and extrinsic muscles of the hand, and the primary wrist muscles were included in the model (Table 2.1). FDS, FDP, and EDC are multi-compartment muscles that are represented by 4 muscle “slips” (e.g. FDS 2, FDS 3, FDS 4, FDS 5) that actuate each digit respectively (McFarland et al., 2023).

4.5 Data Analysis

The TekScan Grip system outputs pressure (kPa) and centre of pressure (grid coordinates) at discrete time points of the collection. Both pressure and centre of pressure for each sensor and the whole hand were provided. Custom code in MATLAB R2022b (MathWorks, Inc., Natick, MA, USA) and Python (Python3.9), was used to extract data needed for inputs into the OpenSim model. Pressure data was averaged for each trial to determine the mean pressure of each sensor. Each sensor's pressure distribution was calculated as a percent of total pressure across all active sensors during each trial. Centre of pressure for each sensor was converted into a distance away from the centre of the sensor (mm) and then averaged across each trial. The force of each trial (in bits) was collected from the force transducer or hand grip dynamometer respectively. Force was converted to Newtons (N) and then filtered using a 2^{nd} order low-pass filter with a frequency cut-off of 6 Hz. Trials were accepted if 90% of the force was in the vertical direction (z- axis). Force distribution was calculated as the product of the filtered Fz during the task multiplied by the previously calculated average pressure distribution of each sensor.

4.5.1 Computing Internal Loads in OpenSim

Custom code in MATLAB was used to conduct the internal loading calculations. The OpenSim model was scaled to each participant's anthropometrics. The Inverse Kinematics tool in OpenSim was used to calculate joint angles from collected marker data. OpenSim uses global optimization to find the coordinates (e.g., joint angles) of the musculoskeletal model that minimizes the difference between the model's markers and experimentally measured marker

data. Physiological constraints to the range of motion for each degree of freedom were added to ensure the solution is realistic to human movement. The elbow was locked in 90 degrees of flexion for all the tasks. The Inverse Dynamics tool was used to calculate net moments for each joint in the fingers and wrist. External forces from the force transducers and the location(s) of point force application from the pressure mapping system were added into the calculation. The Static Optimization tool was used to calculate muscle activation of the wrist and finger musculature. The optimization algorithm minimizes the sum of squared muscle activations. External forces from the force transducers and the location(s) of point force application from the pressure mapping system were added into the calculation.

4.5.2 Input Forces for Simulations

Three different approaches (COM, COP, SP) were used in the computation of internal forces. The COM model distributed the forces over any segment that contributed to the force production and placed loads at each segments center of mass. The COP model distributed the forces over any segment that contributed to the force production and placed loads at each segments centre of pressure. The SP approach placed a single load to mimic the traditional assumptions. The force representation of the SP approach for each task was as follows: For the multi – finger press (MFP) tasks, the force was equally distributed between the fingers involved, with the forces at acting at the centre of mass of the distal tip of the fingers. For the power grips (PG) tasks, a single force was placed at the centre of mass of the hand (head of the third metacarpal). For the Pinch task, the force was equally distributed between all five fingers involved, with the forces at acting at the centre of mass of the distal tip of the fingers. For the single finger press (SFP) tasks, a single force acted at the centre of mass of the distal tip of the

finger. Figure 4.7 provides a visual representation of how the loads were represented in OpenSim.

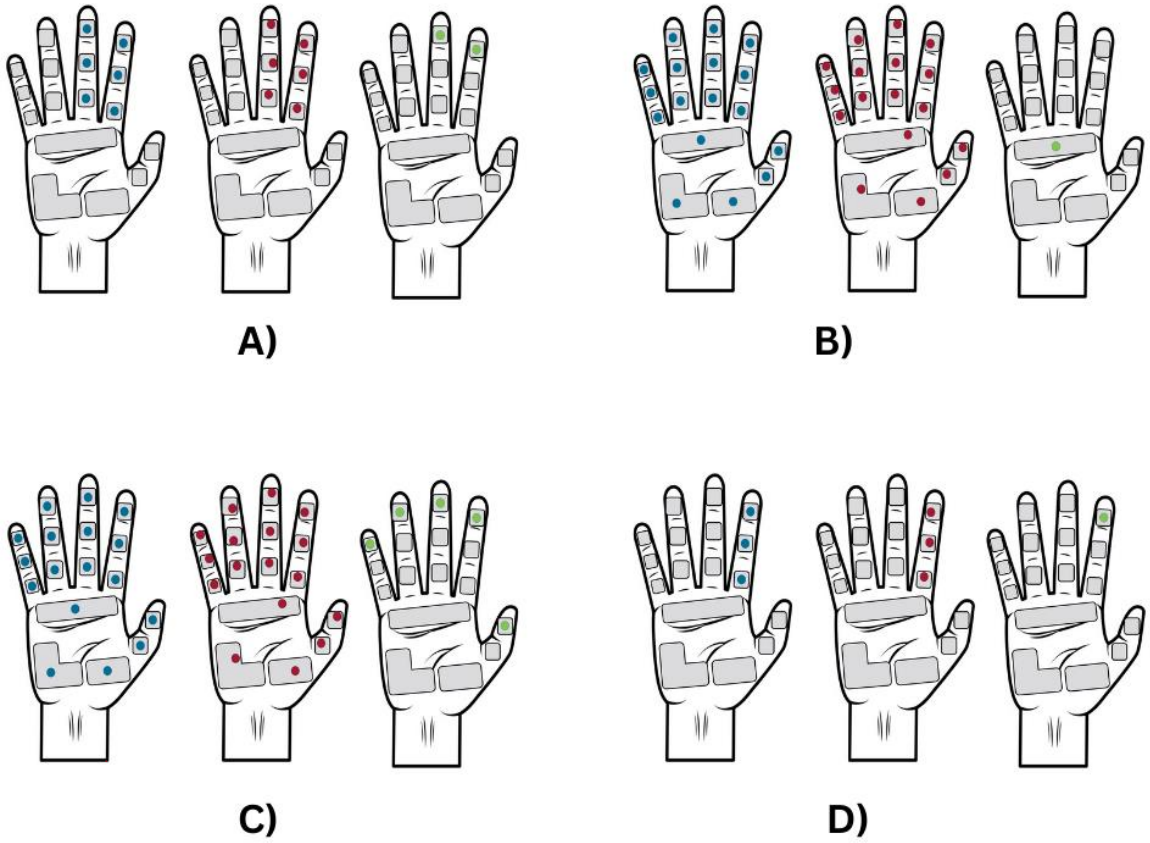

Figure 4.7. A visual representation of load representation for each task (A = MFP23, B = PG, C = Pinch, D = SFP2) in OpenSim. Each hand corresponds to a specific model, blue (COM), red (COP) and green (SP). Points depicted are hypothetical and do not represent actual point of force application.

4.6 Statistical Analysis

Multiple tests of equivalence were conducted in R (V 4.1.1) to assess the effect of how loads are represented (COM, COP, SP) on net joint moments and muscle activations. The data collected did not fit the assumptions to run an analysis of variance. The equivalence test was chosen instead as it examines whether the hypotheses' effects are extreme enough to be

considered meaningful and can be rejected (Lakens et al., 2018), whereas traditional tests of variance only inform differences between groups. An upper and lower equivalence bound is specified based on the smallest effect size of interest and two composite hypotheses are tested. The null hypothesis ($H_{0\,NHST}$) of the classic null hypothesis significance testing (NHST) would be that the means of the two populations are the same. The null hypothesis ($H_{0\,EQ}$) of the equivalence tests (EQ) would be that the difference between the means is outside the established equivalence interval. If both $H_{0\,NHST}$ and $H_{0\,EQ}$ are rejected, the conclusion is that the observed effect falls withing the equivalence bounds and is close enough to zero, and therefore statistically equivalent (Lakens, 2017). There are four interpretations of tests of equivalence based on Lakens et al., (2017), outlined in Table 4.1. Bonferroni corrections were made for both objectives to protect from Type I error.

Table 4.1. Interpretation of tests of equivalence, $\alpha = 0.05$.

Interpretation	Reject $H_{0\,NHST}$ at α?	Reject $H_{0\,EQ}$ at α?
Trivial difference	Reject	Reject
Equivalent	Not reject	Reject
Relevant difference	Reject	Not reject
Indeterminate	Not reject	Not reject

The dependent variables were model outputs (internal net joint moments and muscle activations). The independent variables were model type (COM, COP, and SP). In order to answer research objective 1, a series of equivalence tests was used to assess the effect of model type (COM, and COP compared to the traditional SP model) on model output (internal net joint moments) to identify relevant differences (reject $H_{0\,NHST}$, do not reject $H_{0\,EQ}$) between models. An a priori effect size of $\alpha < 0.05$ and an equivalence interval of 0.01 Nm were selected. Complaints of muscular fatigue, pain and soreness were seen in static muscle activity as low as 2% of their maximum voluntary contraction (Veiersted et al., 1990). Maximum finger press force

with the index finger has been reported to be around 50 N (Keenan & Massey, 2012). If this the force recorded during maximum voluntary contraction, then at 2% of their maximum voluntary contraction, participants would be able to generate 1 N of force and about 0.5 – 1.0 Nm at the MCP joint depending on anthropometrics. At the recorded maximum, a 10% change would be about 0.01 Nm, therefore the equivalence bound was set to this value. To answer research objective 2, the same methodology was applied. With an a priori effect size of $\alpha < 0.05$ and an equivalence interval of 0.02 or 2% of maximum voluntary activation. This equivalence bound was determined as complaints of muscular fatigue, pain and soreness were seen in static muscle activity as low at 2% of their maximum voluntary contraction (Veiersted et al., 1990).

CHAPTER 5

RESULTS

The sensors were used to determine the distribution of force measured by the force transducer. The applied forces were distributed across the sensors based on the task (Table 5.1). Only the sensors of the active digits in each task were used to calculate the percentage on each segment to exclude pressures from incidental contact. During the multi-finger presses, MFP23, MFP234, and MFP2345, the largest percentage of total pressure was found at the distal phalanx of digit 2 (MFP23: 45.6% ± 18%; MFP234: 31.2% ± 17%; MFP2345: 28.1% ± 15%). There were also large percentages of total pressure at the distal phalanx of digit 3 during MFP23, MFP234, MFP2345 (33.7% ± 15%, 30.0% ± 13%, 22.6% ± 8%, respectively). Percentage of total force distributions were lower in all three areas of digit 4 and 5 during MFP234 and MFP2345. Large variability was seen in the proximal phalanx sensors of all active digits where their standard deviations were larger than the means (Table 5.1). During the power grips, PG20 and PG40, the most percent of total pressure was in the middle phalanges of digit 3 (PG20: 16.0% ± 9%; PG40: 15.2% ± 2%), with substantial pressure on all segments of digit 2, 3 and 4. Smaller contributions were in digit 1, digit 5, and the palmar sensors. During the single finger presses, SFP2, SFP3, SFP4 and SFP5, the largest pressure distribution was in the distal phalanges of each active digit (SFP2: 81.0% ± 17%; SFP3: 83.1% ± 18%; SFP4: 76.0% ± 23%; SFP5: 57.3% ± 27%). Interestingly, during SFP5, there were larger contributions from the middle and proximal phalanx (16.5% ± 16%, 26.2% ± 26%) compared to the other single pressing tasks. Pinch had the highest pressure seen in the distal phalanges of digit 2 and 3 (23.3% ± 13%, 23.4% ± 13%). Pinch also had the most variable pressure distribution out of all tasks. This is perhaps due to participants finding it challenging to maintain the 50 N. Throughout all

the tasks, within the participant variability pressure distribution ranged from 0.1% - 4.6% of total pressure (See Appendix B, Table 1).

Table 5.1. Mean (standard deviation) pressure for each sensor for each task across all participants (expressed as percent of sum of pressure on all included sensors).

	Task	MFP23	MFP234	MFP2345	PG20	PG40	SFP2	SFP3	SFP4	SFP5	Pinch
Digit 1	Distal Phalange	-	0.1 (0)	-	2.4 (4)	3.1 (3)	-	-	-	-	3.1 (3)
	Proximal Phalange	-	-	-	1.0 (1)	1.0 (1)	-	-	-	-	1.6 (3)
Digit 2	Distal Phalange	46.5 (18)	31.2 (17)	28.1 (15)	11.2 (8)	12.8 (9)	81 (17)	-	-	-	23.3 (13)
	Middle Phalange	5.0 (8)	3.7 (6)	2.6 (2)	10.2 (6)	10.9 (8)	11.5 (12)	-	-	-	7.7 (8)
	Proximal Phalange	5.3 (9)	4.3 (8)	2.4 (4)	13.1 (12)	11.5 (10)	7.5 (12)	-	-	-	1.4 (1)
Digit 3	Distal Phalange	33.7 (15)	30.0 (13)	22.6 (8)	9.7 (6)	10.4 (6)	-	83.1 (18)	-	-	23.4 (13)
	Middle Phalange	6.3 (12)	4.5 (9)	4.6 (7)	16.0 (9)	15.2 (7)	-	8.9 (9)	-	-	4.3 (5)
	Proximal Phalange	3.1 (5)	3.8 (6)	3.9 (7)	7.0 (5)	6.0 (4)	-	7.9 (11)	-	-	2.0 (2)
Digit 4	Distal Phalange	-	14.0 (9)	14.5 (6)	6.0 (4)	5.5 (4)	-	-	76.0 (23)	-	13.3 (6)
	Middle Phalange	-	6.2 (8)	4.5 (5)	10.4 (6)	10.6 (6)	-	-	14.2 (18)	-	4.9 (5)
	Proximal Phalange	-	2.2 (4)	2.2 (3)	3.3 (2)	3.5 (2)	-	-	9.8 (10)	-	3.1 (5)
Digit 5	Distal Phalange	-	-	9.1 (8)	2.6 (3)	2.8 (2)	-	-	-	57.3 (27)	6.7 (7)
	Middle Phalange	-	-	4.1 (4)	1.7 (1)	1.8 (2)	-	-	-	16.5 (16)	3.0 (2)
	Proximal Phalange	-	-	1.3 (4)	1.3 (1)	1.5 (1)	-	-	-	26.2 (26)	0.7 (1)
Palm	Hypothenar Region	-	-	-	1.7 (1)	1.6 (1)	-	-	-	-	0.5 (0)
	Metacarpal Region	-	-	-	1.2 (1)	1.8 (1)	-	-	-	-	0.6 (0)
	Thenar Region	-	-	-	0.2 (0)	0.2 (0)	-	-	-	-	0.5 (1)
Sum		100	100	100	100	100	100	100	100	100	100

Objective 1 assessed the effect of model type; centre of mass (COM), centre of pressure (COP), and single point (SP) on the computation of internal net joint moments. Objective 2, assessed the effect of model type, COM, COP, and SP on the computation of muscle activity. Equivalence tests were conducted for SP-COM, SP-COP, and COM-COP comparisons. All COM-COP comparisons for both objectives were equivalent (i.e., did not reject $H_{0\,NHST}$ (Null Hypothesis Significance Testing) at α, reject $H_{0\,EQ}$ (Equivalence Testing) at α) and therefore considered practically and statistically the same. Net joint moments and muscle activations between the two models (COM and COP) can be considered the same. This results section will only report statistically relevant differences (i.e., reject $H_{0\,NHST}$ at α, did not reject $H_{0\,EQ}$ at α) for SP-COM (See Appendix B, Table B2) and SP-COP (See Appendix B, Table B3) comparisons.

5.1. Internal Net Joint Moments - OpenSim

5.1.1. Multiple Finger Press - Net Joint Moments

For MFP23 (press with digits 2 & 3), the SP-COM and SP-COP comparisons had relevant differences for all joint moments: DIP flexion, PIP flexion, MCP flexion, and MCP abduction [Equivalence test (EQ) ($p = 0.9 – 0.99$); Null hypothesis significance testing (NHST) ($p < 0.01$)] (Figure 5.1) In digit 2, COP and COM had higher MCP flexion and abduction moments, and lower PIP and DIP flexion moments when compared to SP. In digit 3, SP was higher in all moments.

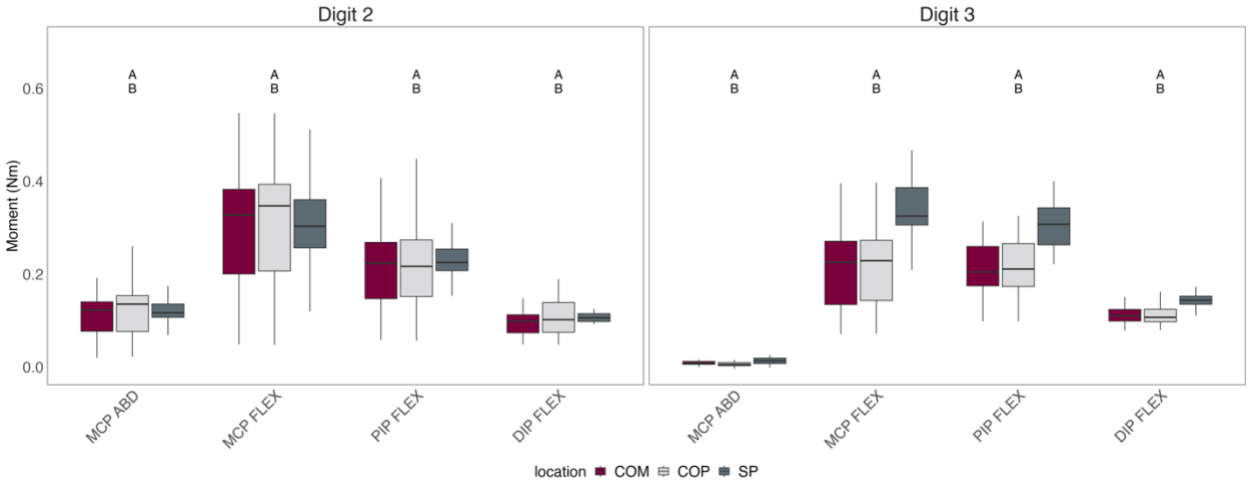

Figure 5.1. MFP23 (15 N). Box and whisker plots depicting net joint moments for digit 2 (left) and 3 (right). Horizontal lines represent the median joint moment; box limits = upper and lower quartiles; whiskers = range. "A" = relevant difference between the COM-SP comparisons. "B" = relevant difference between the COP-SP comparisons. Positive moments are abduction and flexion.

For MFP234 (press with digits 2 to 4), the SP-COM and SP-COP comparisons had relevant differences for all joint moments [EQ ($p = 0.64 – 0.93$); NHST ($p < 0.01$)] (Figure 5.2). In digit 2, SP was highest for MCP abduction, PIP and DIP flexion moments, but COP had higher MCP flexion. In digit 3, SP had the lowest MCP abduction and flexion moments, but highest PIP and DIP flexion moments. For digit 4, SP calculated lower MCP abduction and the highest MCP, PIP and, DIP flexion moments when compared to COM and COP.

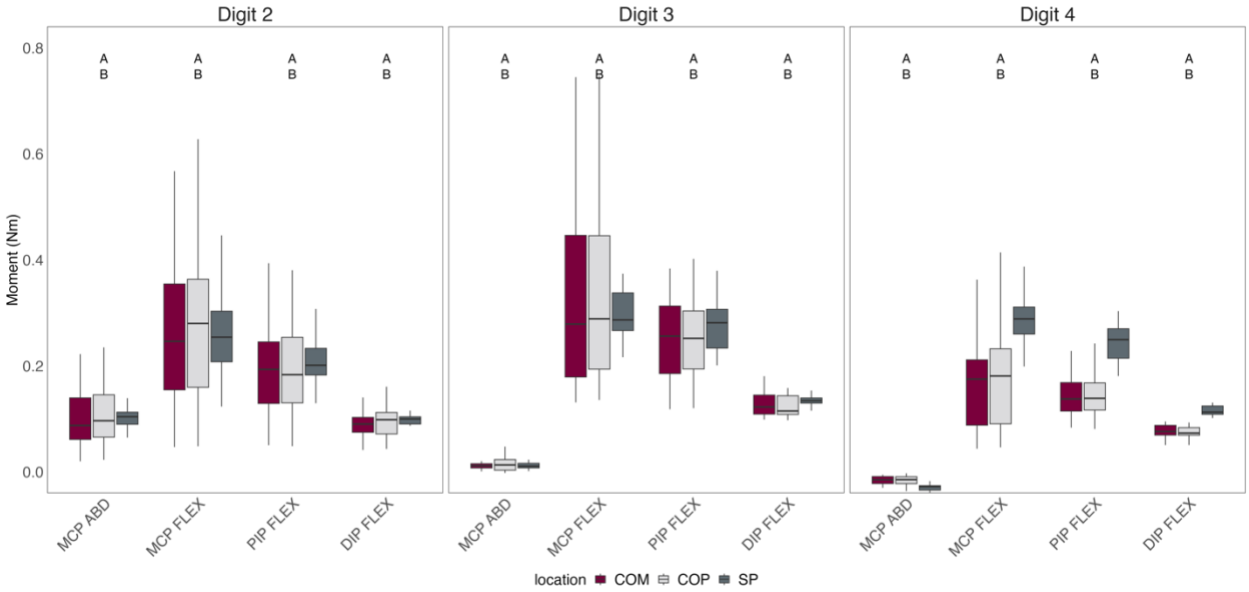

Figure 5.2. MFP234 (20 N). Box and whisker plots depicting net joint moments for digit 2 (left) to 4 (right). Horizontal lines represent the median joint moment; box limits = upper and lower quartiles; whiskers = range. "A" = relevant difference between the COM-SP comparisons. "B" = relevant difference between the COP-SP comparisons. Positive moments are abduction and flexion.

For MFP2345 (press with digits 2 to 5), the SP-COM comparison had relevant differences for all joint moments [EQ ($p = 0.38$); NHST ($p < 0.01$)] (Figure 5.3). In digit 2, SP had the lowest for all moments compared to COM and COP. In digits 3, 4 and 5, SP had the lowest MCP abduction but, the highest MCP, PIP and DIP flexion moments out of all three models.

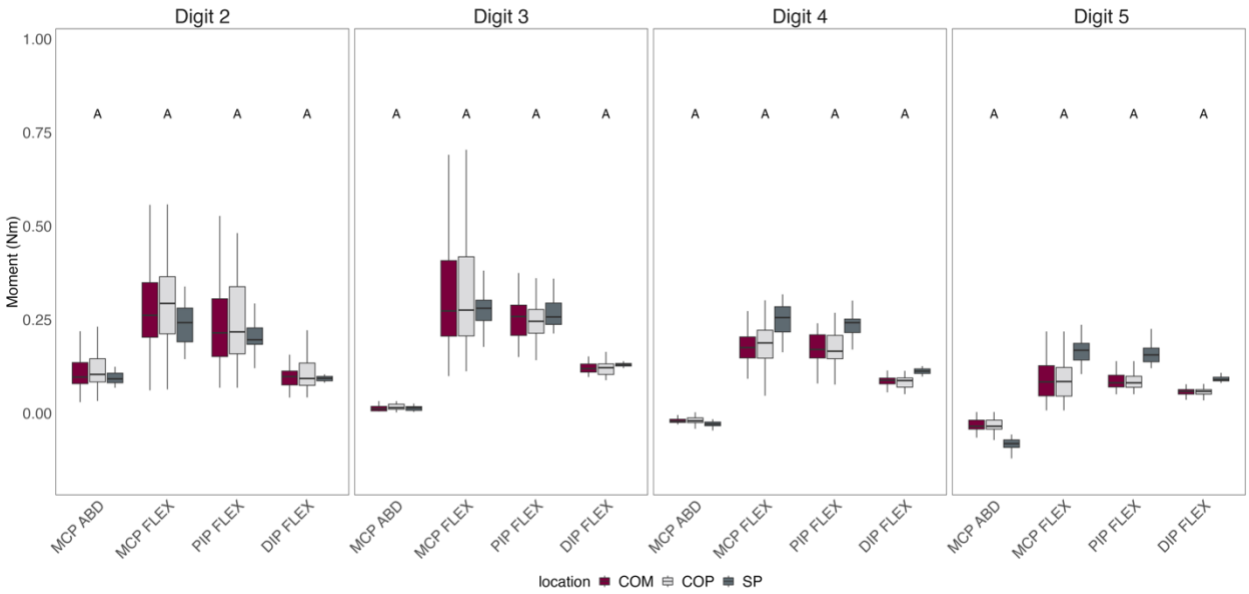

Figure 5.3. MFP2345 (25 N). Box and whisker plots depicting net joint moments for digit 2 (left) to 5 (right). Horizontal lines represent the median joint moment; box limits = upper and lower quartiles; whiskers = range. "A" = relevant difference between the COM-SP comparisons. "B" = relevant difference between the COP-SP comparisons. Positive moments are abduction and flexion.

5.*1.2. Power Grip - Net Joint Moments*

During PG20, the SP-COM and SP-COP comparisons had relevant differences for all joint moments, DIP flexion, PIP flexion, MCP flexion and MCP abduction [EQ ($p = 1.0$); NHST ($p < 0.01$)] (Figure 5.4A). In the thumb (digit 1), SP generated the highest moments for MCP abduction, and the lowest MCP, PIP and DIP flexion moments. For digit 2 and 3, SP had the lowest moments out of all three models. In digit 4 and 5, SP had the highest MCP abduction and had the lowest flexion moments for MCP, PIP, and DIP. During PG40, the SP-COM comparison had relevant differences for all joint moments [EQ ($p = 1.0$); NHST ($p < 0.01$)] (Figure 5.4B). In digit 1, SP had lower MCP abduction, PIP and DIP flexion moments, but the larger MCP flexion moment compared to COM. For digit 2, 3, 4, and 5, SP had the lowest moments compared to COM and COP. All moments were larger in PG40 than PG20.

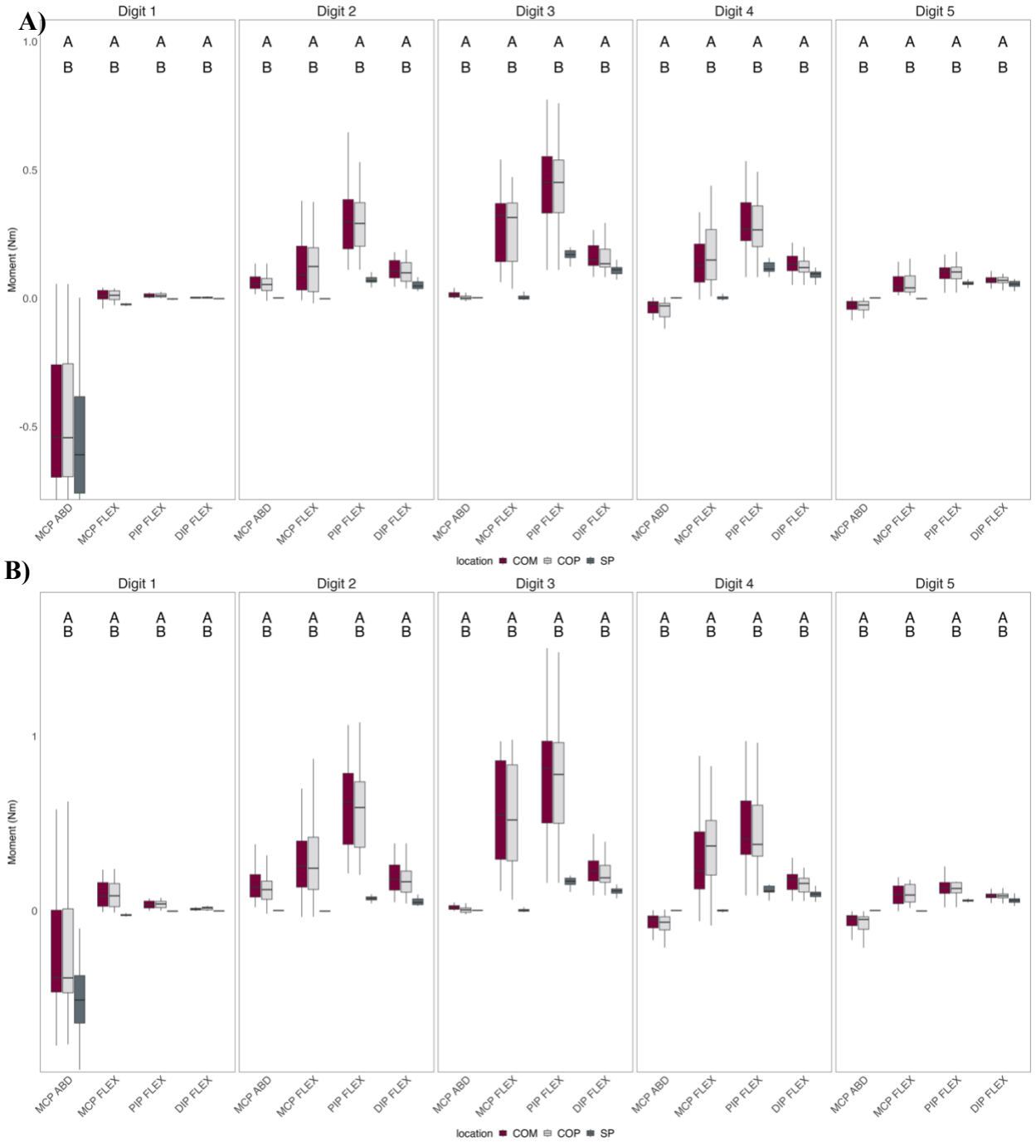

Figure 5.4. A) PG20 (20% MVG) and B) PG40 (40% MVG). Box and whisker plots depicting all net joint moments for digit 1 (left) to 5 (right). Horizontal lines represent the median moment; box limits = upper and lower quartiles; whiskers = range. "A" = relevant difference between the COM-SP comparisons. "B" = relevant difference between the COP-SP comparisons. Positive moments are abduction and flexion.

5.1.3. Pinch - Net Joint Moments

For Pinch, the SP-COM comparison had relevant differences for all joint moments, DIP flexion, PIP flexion, MCP Flexion and MCP abduction [EQ ($p = 0.93$); NHST ($p < 0.01$)] (Figure 5.5). In digit 1, SP was highest in all moments. In digit 2 and 3, SP was the lowest for all moments. In digit 4 and 5, SP was higher for all moments compared to COM.

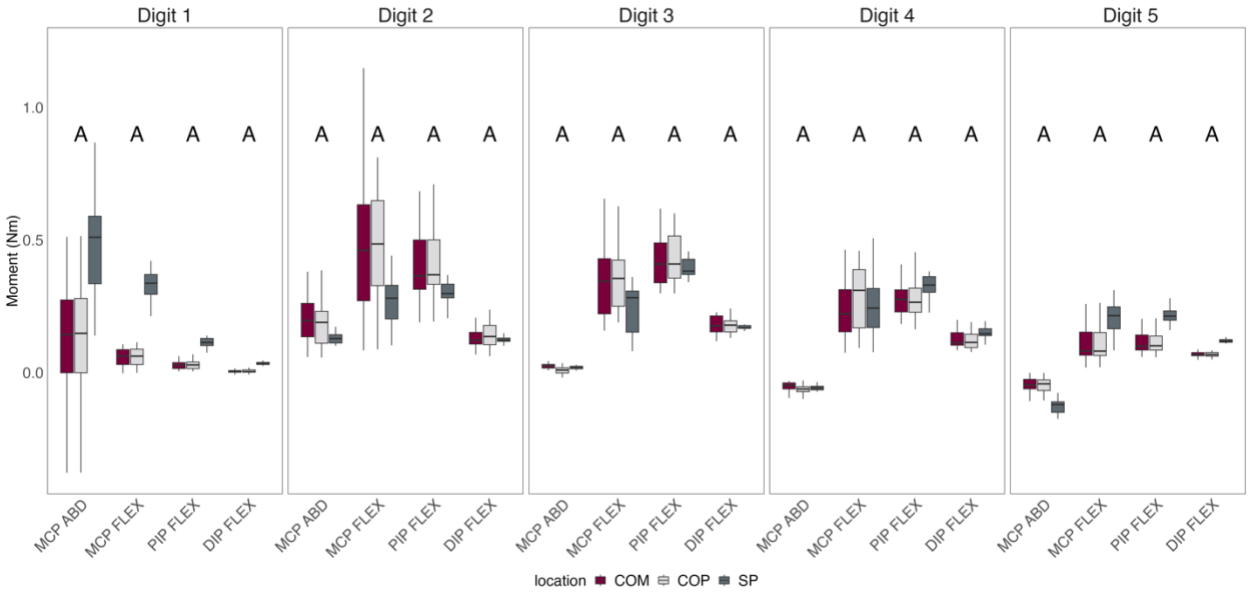

Figure 5.5: Pinch grip (50 N). Box and whisker plots depicting all net joint moments for digit 1 (left) to 5 (right). Horizontal lines represent the median moment; box limits = upper and lower quartiles; whiskers = range. "A" = relevant difference between the COM-SP comparisons. "B" = relevant difference between the COP-SP comparisons. Positive moments are abduction and flexion.

Throughout all tasks that have multiple digits that contribute to the force distribution (MFP, PG, and Pinch), digits 4 and 5 had larger moments with the SP when compared to COM and COP. There was also larger variability in COM and COP outputs compared to SP for these tasks. This was most likely due to the inclusion of force distributions in COM and COP, where majority of the forces across the entire hand came from digit 2 and 3 during these tasks.

5.1.4. Single-Finger Press - Net Joint Moments

For all single finger pressing tasks (SFP2, SFP3, SFP4, SFP5) the SP-COM and SP-COP comparisons had relevant differences for all joint moments, DIP flexion, PIP flexion, MCP Flexion and MCP abduction [EQ ($p = 1.0$); NHST ($p < 0.01$)] (Figure 5.6a, Figure 5.6b, Figure 5.6c, Figure 5.6d,). At the active digit for each single finger press, SP had larger MCP abduction and MCP, PIP and DIP flexion moments compared to COM and COP.

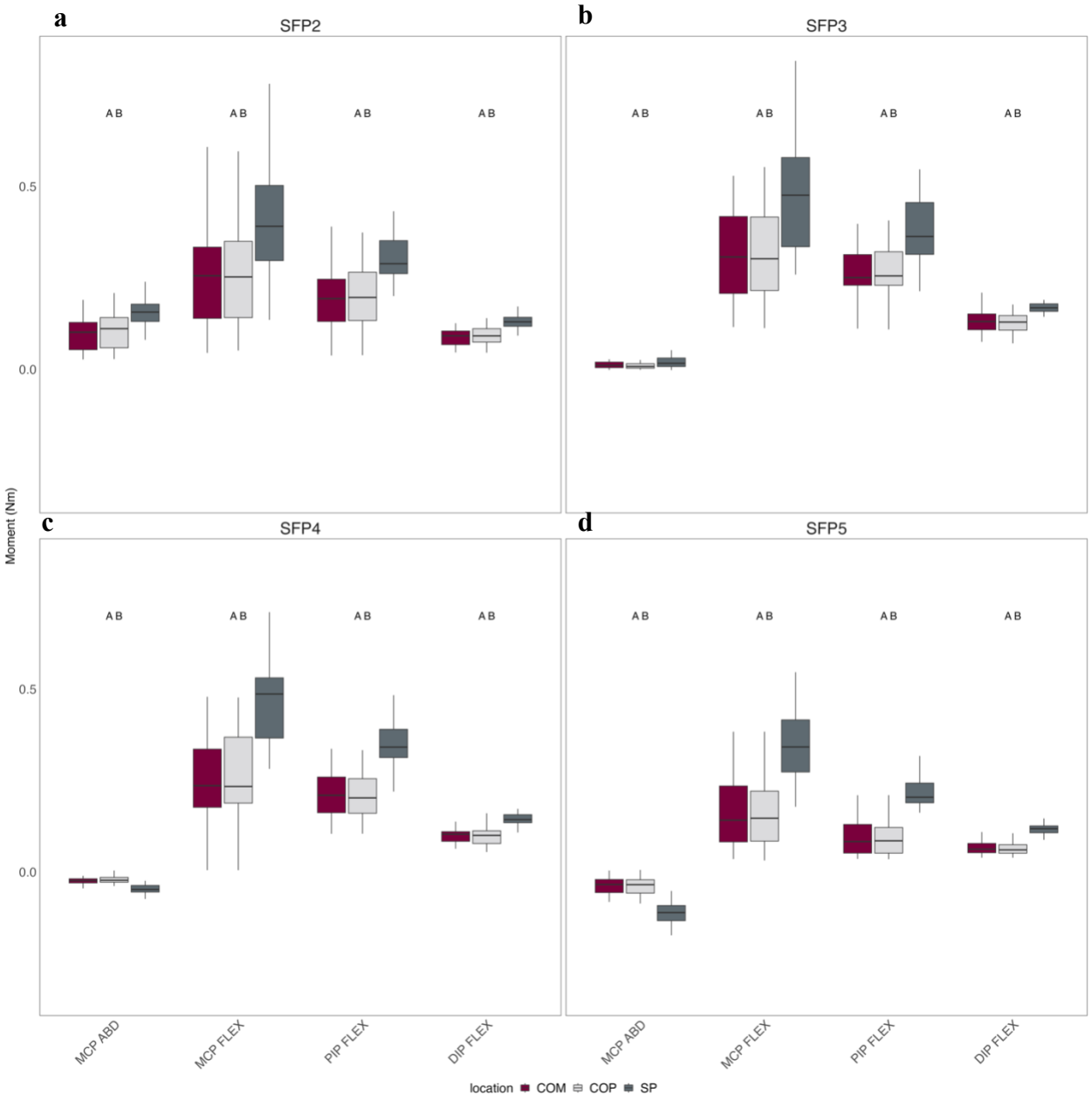

Figure 5.6. a (SFP2), b (SFP3), c (SFP4), d (SFP5) (10 N) Box and whisker plots depicting all net joint moments for digit 1 (left) to 5 (right). Horizontal lines represent the median moment; box limits = upper and lower quartiles; whiskers = range. "A" = relevant difference between the COM-SP comparisons. "B" = relevant difference between the COP-SP comparisons. Positive moments are abduction and flexion.

5.2. Muscle Activations - OpenSim

5.2.1. Multiple Finger Press Muscle Activations

For MFP23, SP had higher muscle activities for FDS 3, FDP 2, and FDP 3 compared to COM [EQ ($p = 0.8 – 1.0$); NHST ($p < 0.001$)] (Figure 5.7). The SP-COP comparison had the same result, including SP higher FDS 2 activations, and ECU having the highest activation with COP [EQ ($p = 0.1 – 1.0$); NHST ($p < 0.001$)] (Figure 5.7).

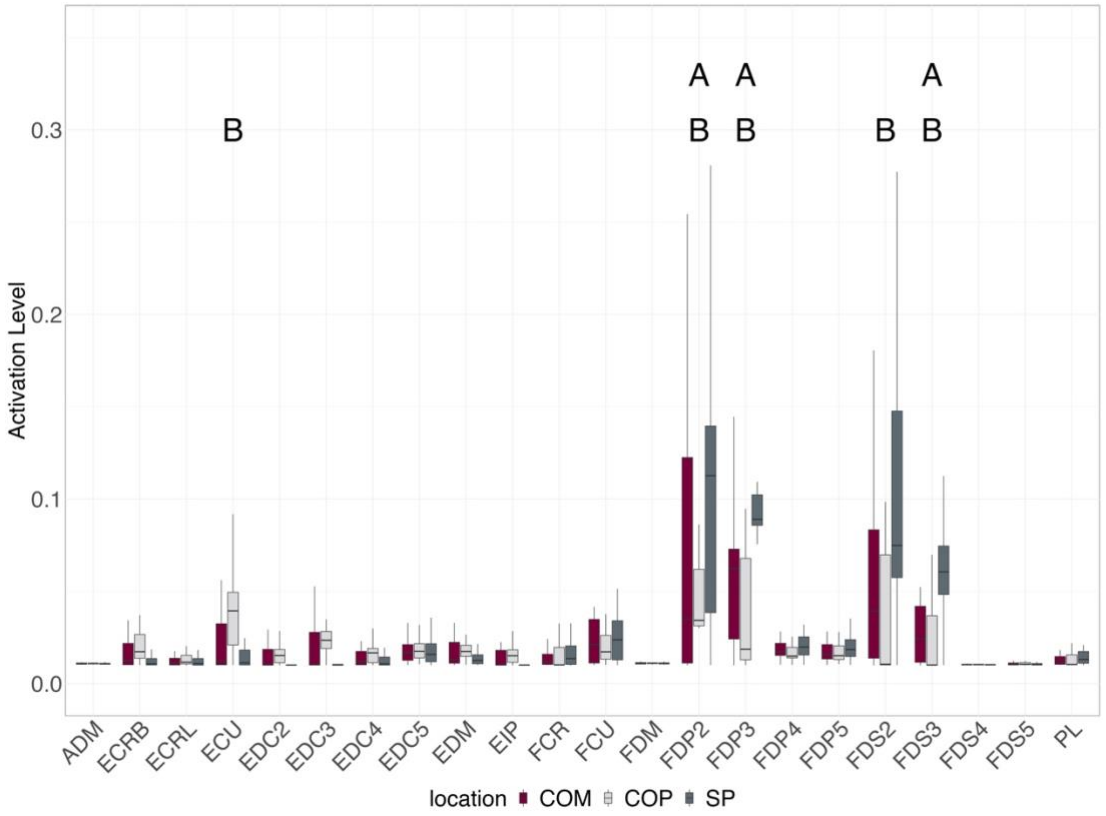

Figures 5.7. MFP23 (15 N). Box and whisker plots depicting muscle activity or forearm and finger musculature. Horizontal lines represent the median muscle activity; box limits = upper and lower quartiles; whiskers = range. "A" = relevant difference between the COM-SP comparisons. "B" = relevant difference between the COP-SP comparisons.

For MFP234, the SP comparison had higher activations than COM and COP for FDP 3, FDP 4, and FDS 5 [EQ ($p = 0.5 – 1.0$); NHST ($p < 0.001$)] (Figure 5.8). SP also had higher activations for FDP 2, FDS 2, FDS 3, and FDS 4 [EQ ($p = 0.01 – 1.0$); NHST ($p < 0.001$)] than COP (Figure 5.8). ECU had the largest activity with COP EQ ($p = 0.1$); NHST ($p < 0.001$)].

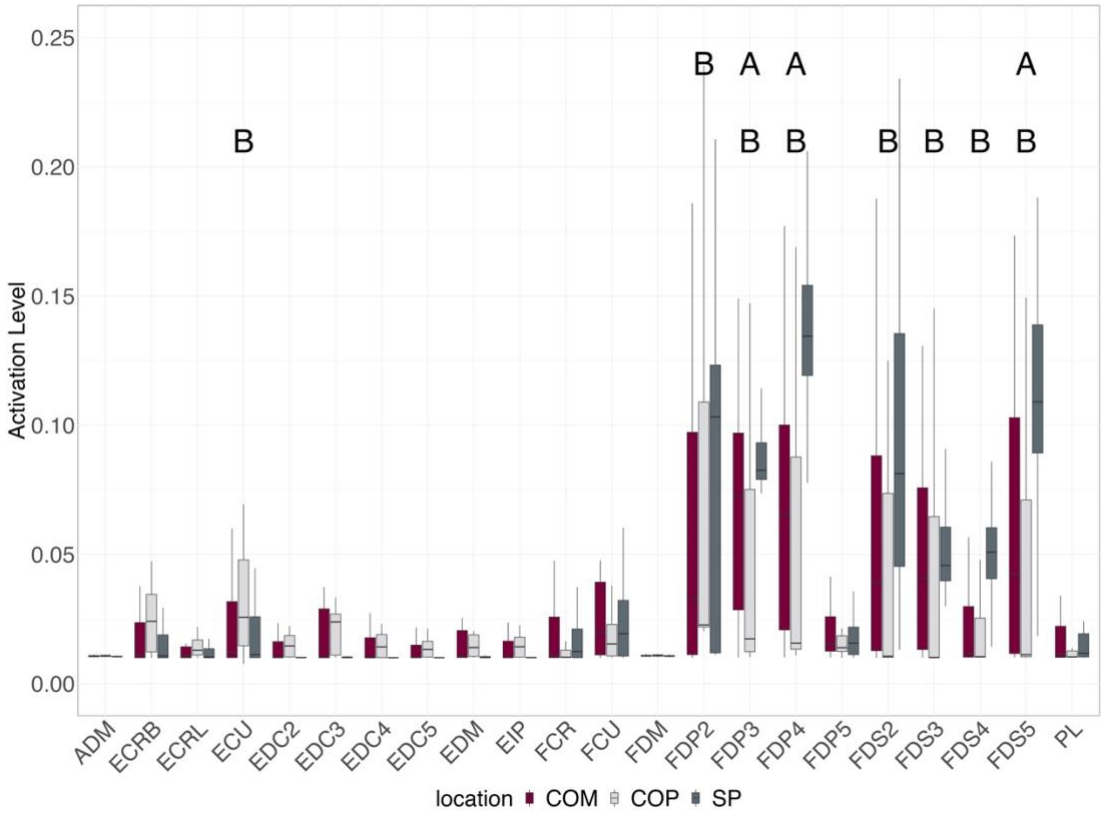

Figures 5.8. MFP234 (20 N) Box and whisker plots depicting muscle activations. Horizontal lines represent the median muscle activity; box limits = upper and lower quartiles; whiskers = range. "A" = relevant difference between the COM-SP comparisons. "B" = relevant difference between the COP-SP comparisons.

For MFP2345, the SP had larger activations than COM and COP for FDP 3, FDP 4, and FDP 5 [EQ ($p = 0.8 – 1.0$); NHST ($p < 0.001$)] (Figure 5.9). SP had higher FDS 5 activations than COM as well as higher FDP 2 and FDS 2 activations compared to COP [EQ ($p = 0.96 – 1.0$); NHST ($p < 0.001$)] (Figure 5.9).

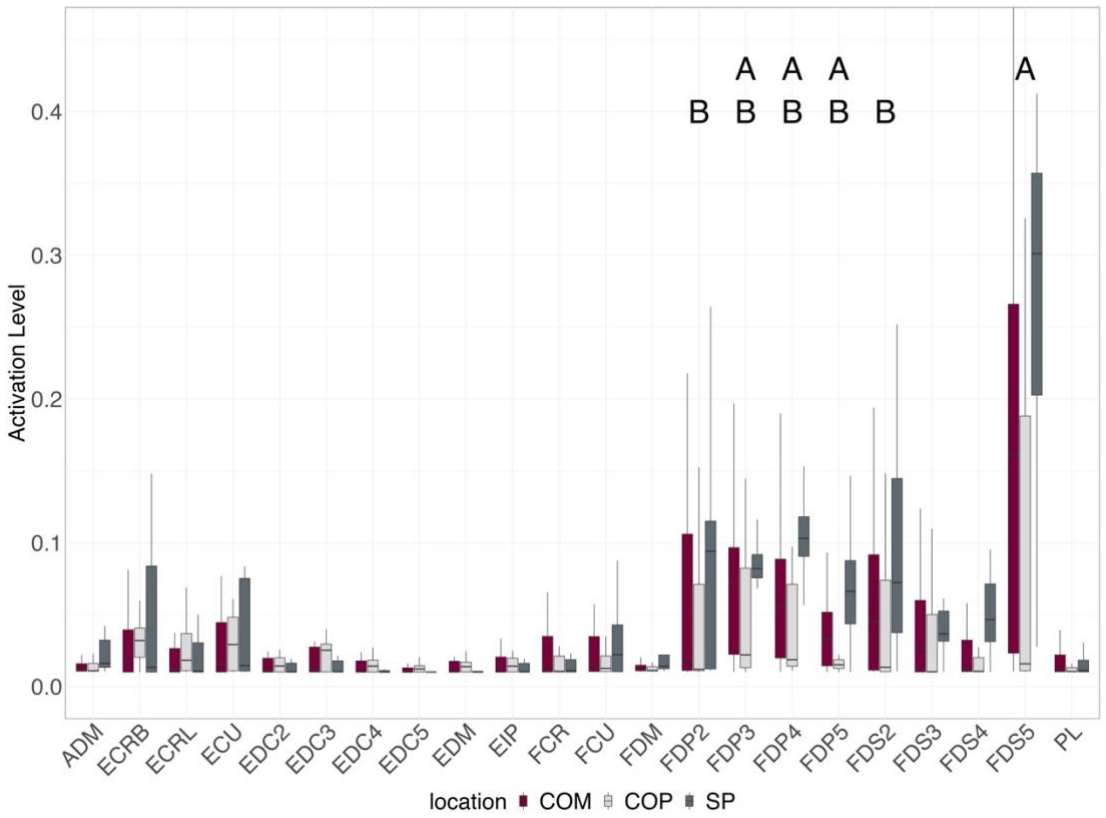

Figures 5.9. MFP2345 (25 N). Box and whisker plots depicting muscle activity or forearm and finger musculature. Horizontal lines represent the median muscle activity; box limits = upper and lower quartiles; whiskers = range. "A" = relevant difference between the COM-SP comparisons. "B" = relevant difference between the COP-SP comparisons.

All multi-finger presses had larger variability in the finger flexor activity of the compartments of the active digits (FDP 2, FDP 3, FDP 4, etc.) likely due to the contributions from the force distributions. As the number of active digits and force level increases, activations stayed about the same. Unexpectedly, ECU activation was higher in COP than SP during MFP23 and MFP234.

5.2.2. Power Grip - Muscle Activations

For PG20, both COM and COP had higher ECRB, ECRL, and ECU activations and lower FCR, FCU, FDP 5, and PL activations compared to SP [EQ ($p = 0.4 – 1.0$); NHST ($p <$

0.001)] (Figure 5.10). EDM activation was higher in COM than SP [EQ (p = 0.98); NHST (p < 0.001)]. The SP had higher FPL, and APL muscle activations [EQ (p = 0.02 – 0.92); NHST (p < 0.001)] compared to SP.

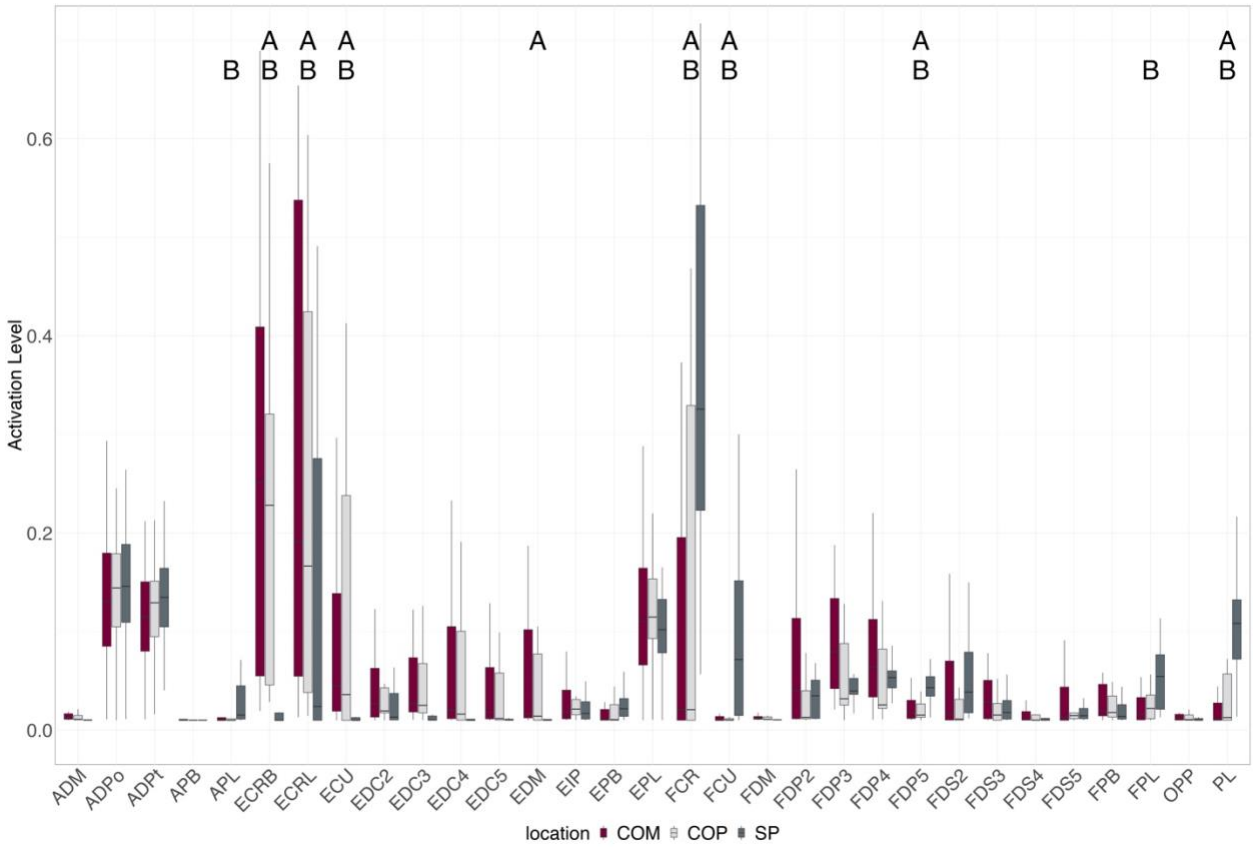

Figures 5.10. PG20 (20% MVG) Box and whisker plots depicting muscle activity or forearm and finger musculature. Black horizontal lines represent the median muscle activity; box limits = upper and lower quartiles; whiskers = range. "A" = relevant difference between the COM-SP comparisons. "B" = relevant difference between the COP-SP comparisons.

For PG40, both COM and COP had higher activations for ECRL, ECRB, ECU, and lower FCU, PL, FDS 5, FPL, and ADPt muscle activations [EQ (p = 0.9 – 1.0); NHST (p < 0.001)] (Figure 5.11). In addition, COM comparison had larger EDC 2, EDC 3, EDC 4, EDC 5, EDM, FDP 2 and FDP 3 muscle activations compared to SP [EQ (p = 0.9- 1.0); NHST (p < 0.001)]. The SP had larger activations of EPB and FDS 2, and lower EPL activation compared to COP [EQ (p = 0.8 – 0.9); NHST (p < 0.001) (Figure 5.11). With both exertion levels, there is larger

activity and variability in extensor activity for COM and COP compared to the flexors. As the level of exertion increases, activations naturally increase as well.

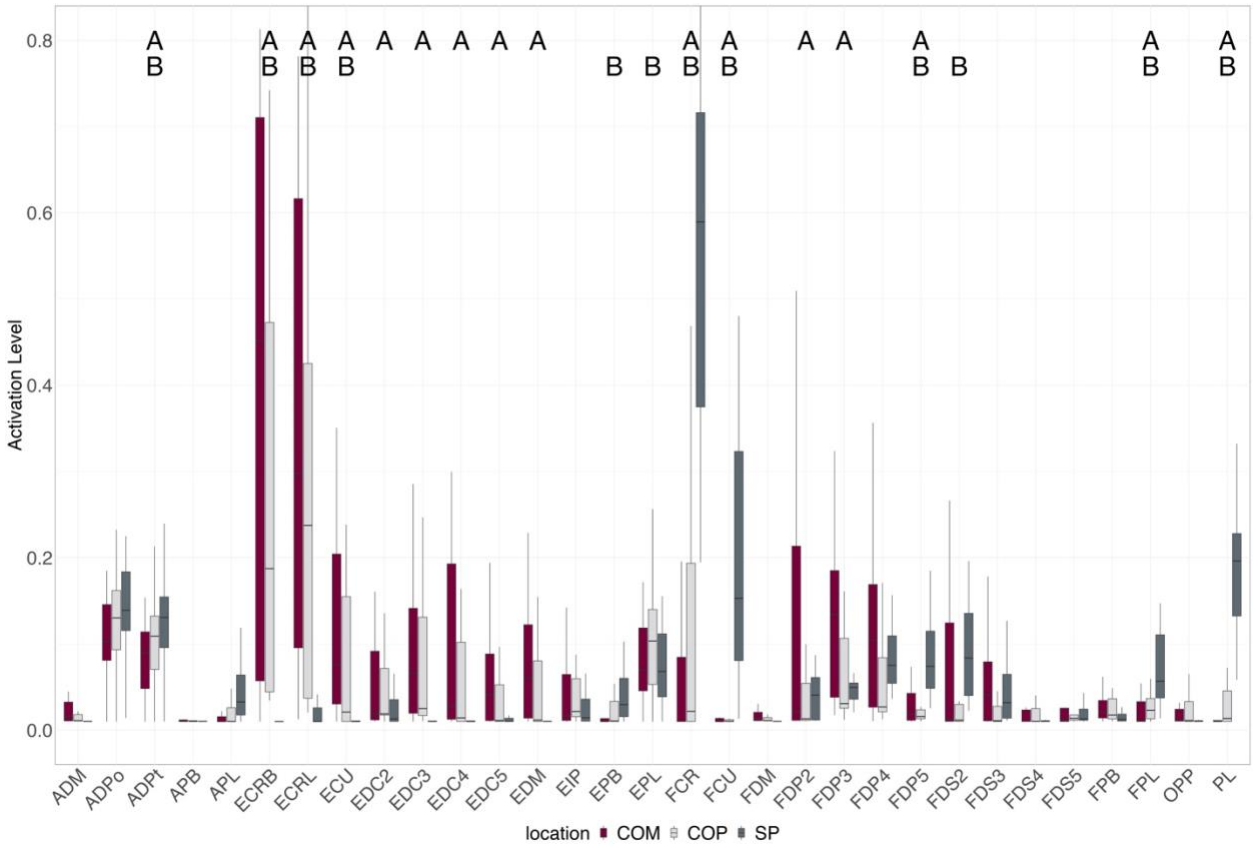

Figures 5.11. PG40 (40% MVG) Box and whisker plots depicting muscle activity or forearm and finger musculature. Black horizontal lines represent the median muscle activity; box limits = upper and lower quartiles; whiskers = range. "A" = relevant difference between the COM-SP comparisons. "B" = relevant difference between the COP-SP comparisons.

5.2.3. Pinch - Muscle Activations

For the Pinch task, SP had higher activations for FDP 5, FDP 4, and OPP compared to both COM and COP [EQ ($p = 0.98 – 1.0$); NHST ($p < 0.001$)] (Figure 5.12). The SP had higher FDP 2, FDP 3, FDS 2, FDS 3, FDS 4, FDS5, FPB and FPL muscle activations than COP [EQ (p

= 0.02 – 0.92); NHST ($p < 0.001$)]. COP had higher ECRL activation than SP [EQ ($p = 0.92$); NHST ($p < 0.001$)]. There were large amounts of activation from both flexors and extensors. Amongst all tasks, Pinch was the most variable in terms of activation levels, due to the challenge of maintaining a 50 N pinch force.

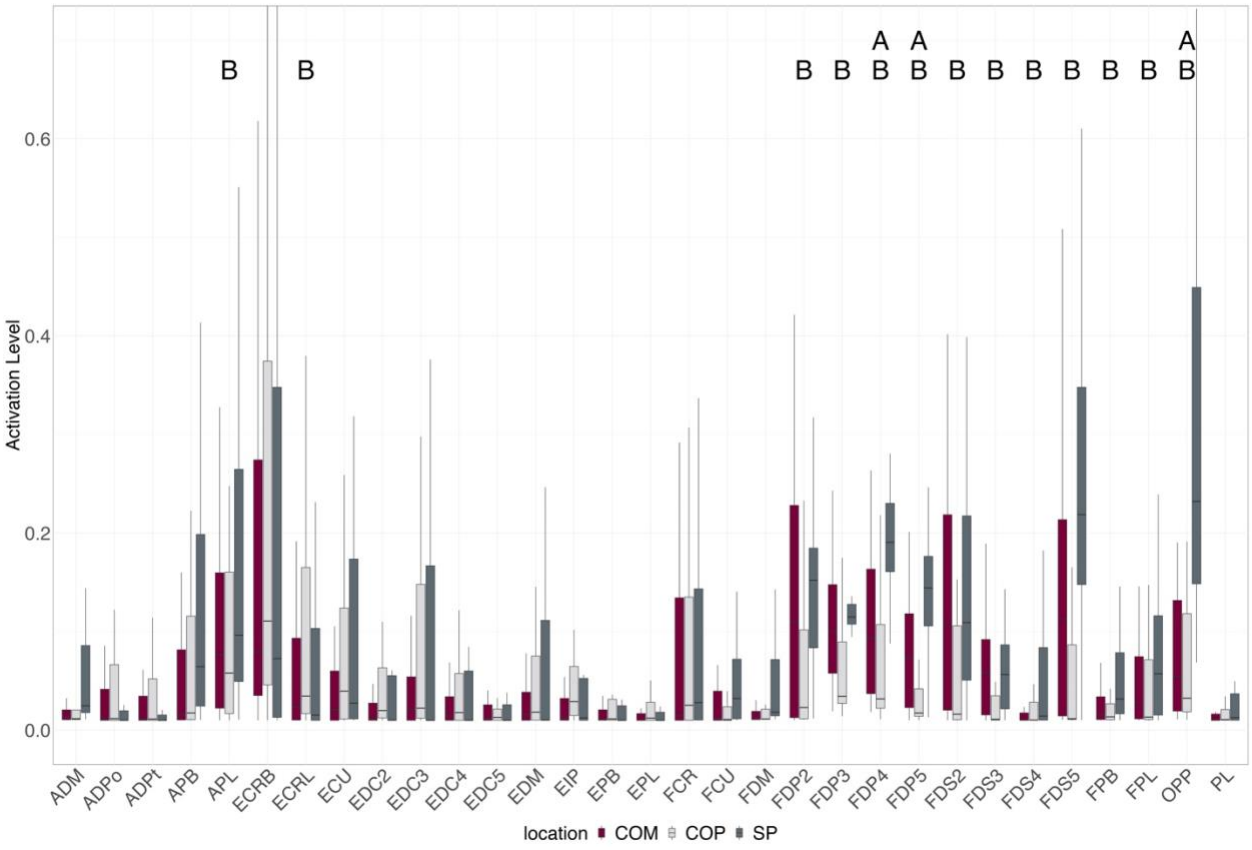

Figure 5.12. Pinch (50 N) Box and whisker plots depicting muscle activity or forearm and finger musculature. Black horizontal lines represent the median muscle activity; box limits = upper and lower quartiles; whiskers = range. "A" = relevant difference between the COM-SP comparisons. "B" = relevant difference between the COP-SP comparisons.

5.2.4. Single-Finger Press - Muscle Activity

For SFP2, SP had higher activations for FDS 2 and FDP 2 compared to both COM and COP [EQ ($p = 1.0$); NHST ($p < 0.001$)] (Figure 5.13). In addition, COP had higher ECU muscle activation than SP [EQ ($p = 0.43$); NHST ($p < 0.001$)].

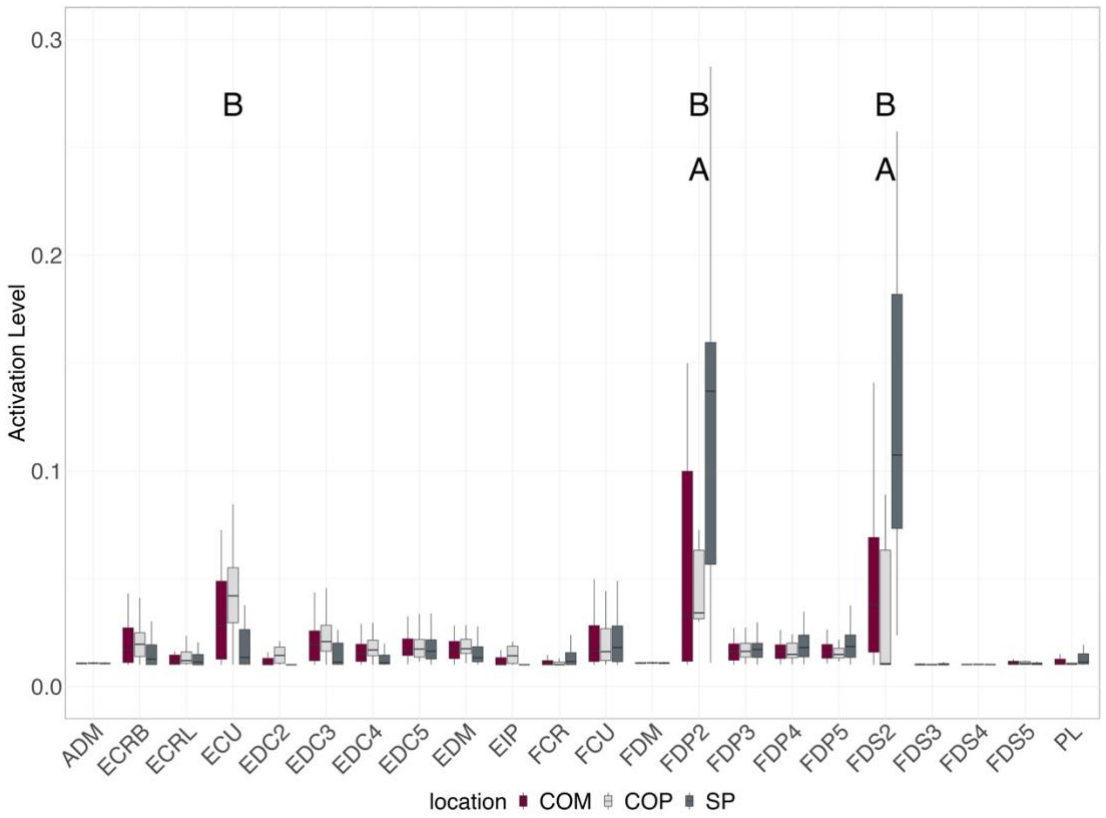

Figure 5.13: SFP2 (10 N) Box and whisker plots depicting muscle activity or forearm and finger musculature. Black horizontal lines represent the median muscle activity; box limits = upper and lower quartiles; whiskers = range. "A" = relevant difference between the COM-SP comparisons. "B" = relevant difference between the COP-SP comparisons.

For SFP3, SP had higher activations for FDS 3, and FDP 2 muscle activations compared to COM and COP [EQ ($p = 1.0$); NHST ($p < 0.001$)] (Figure 5.14). COP had higher ECU and EDC 3 muscle activations than SP [EQ ($p = 0.3 – 1.0$); NHST ($p < 0.001$)].

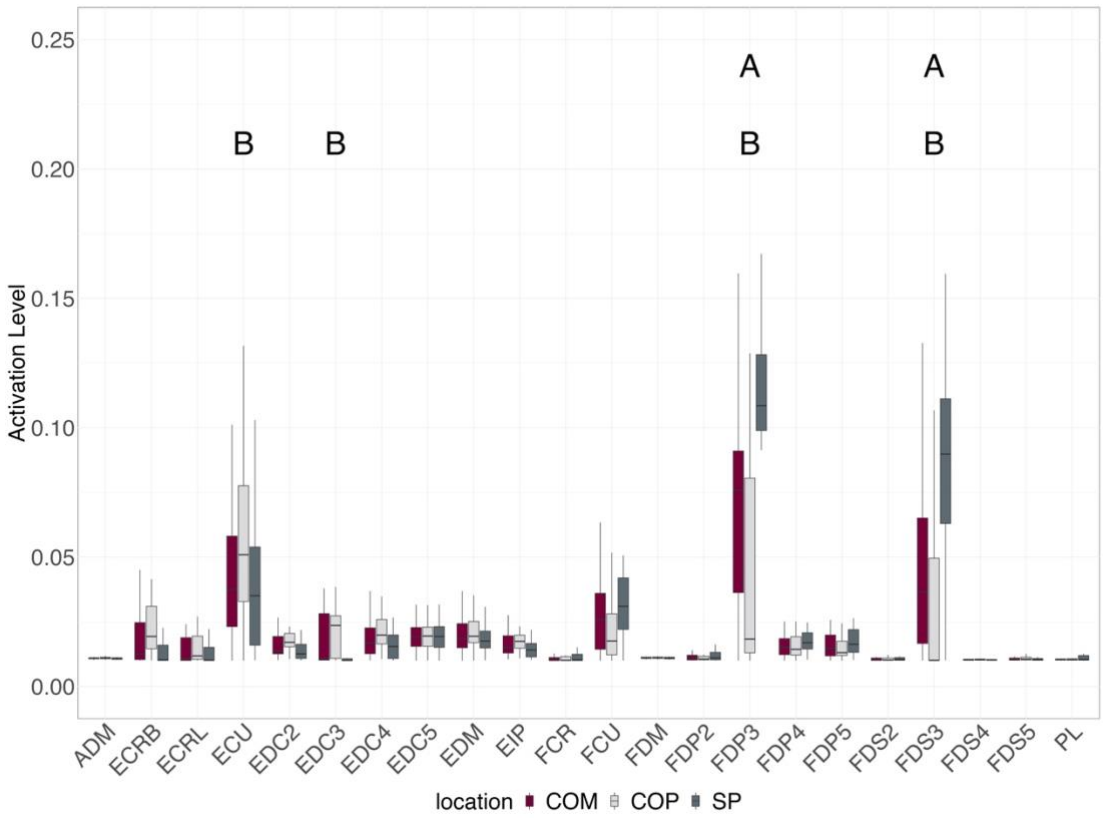

Figure 5.14. SFP3 (10 N) Box and whisker plots depicting muscle activity or forearm and finger musculature. Black horizontal lines represent the median muscle activity; box limits = upper and lower quartiles; whiskers = range. "A" = relevant difference between the COM-SP comparisons. "B" = relevant difference between the COP-SP comparisons.

For SFP4, SP had higher activations for FDS 5, FDS 4 and FDP 4 compared to both COM and COP [EQ ($p = 1.0$); NHST ($p < 0.001$)] (Figure 5.15).

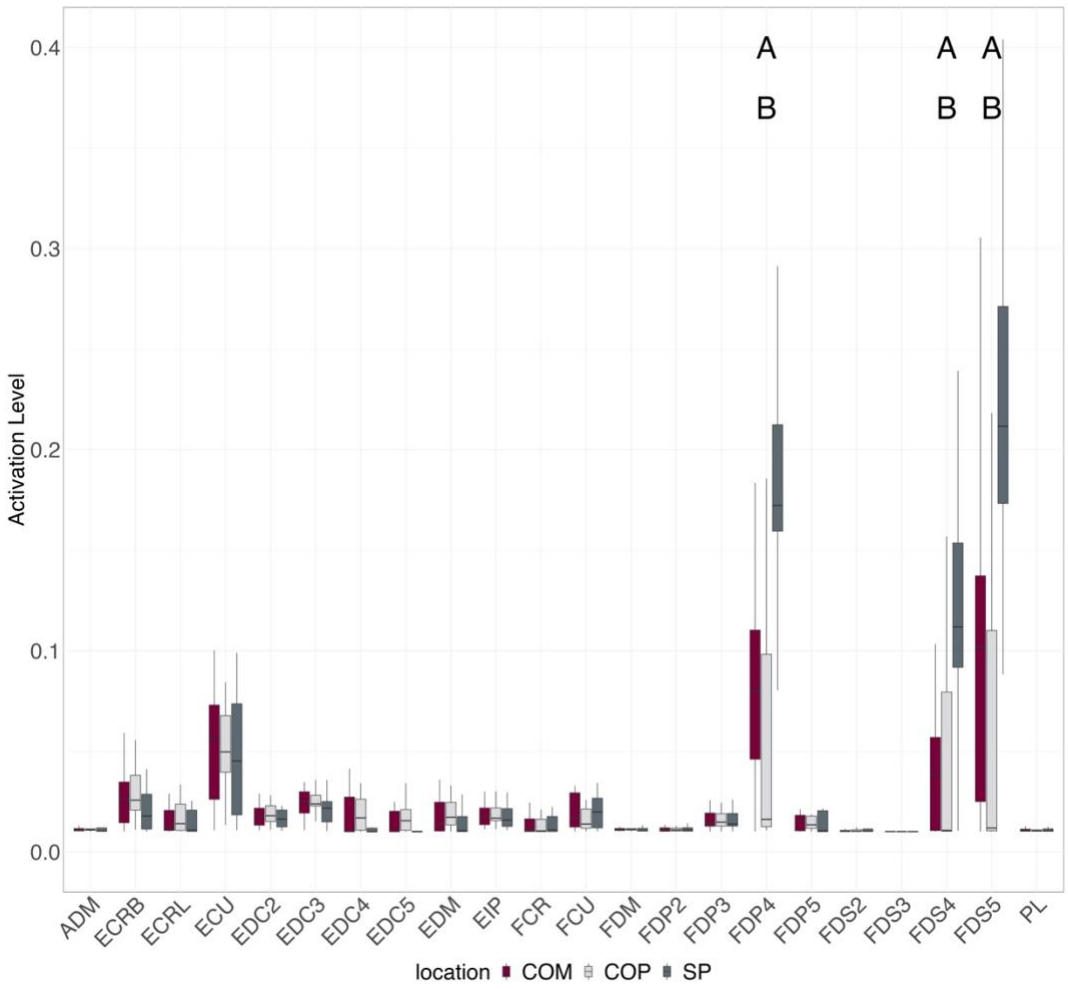

Figure 5.15. SFP4 (10 N) Box and whisker plots depicting muscle activity or forearm and finger musculature. Black horizontal lines represent the median muscle activity; box limits = upper and lower quartiles; whiskers = range. "A" = relevant difference between the COM-SP comparisons. "B" = relevant difference between the COP-SP comparisons.

For SFP5, SP had higher activations for ECU, FDP 5, ADM compared to COM and COP [EQ ($p = 0.9$- 1.0); NHST ($p < 0.001$)] (Figure 5.16). In addition, the SP had higher FDS 3, FDP 3, AND FDM muscle activations than COM [EQ ($p = 0.4 – 1.0$); NHST ($p < 0.001$)]. The SP had higher activations for FCU, PL, FDP 2, and EDC 3 muscle activations compared to COP [EQ ($p = 0.9 – 1.0$); NHST ($p < 0.001$)]. SFP5 had higher activity with large amounts of variability in all muscles when computed with SP. Throughout all the SP tasks, the largest variability in activity was in the finger flexor compartments of each respective task (FDS 2 and FDP 2 during SFP2,

FDS 3 and FDP 3 during SFP3, FDS 4 and FDP 4 during SFP4, FDS 5 and FDP 5 during SFP5).

The compartments also had larger activity computed with SP compared to COM and COP.

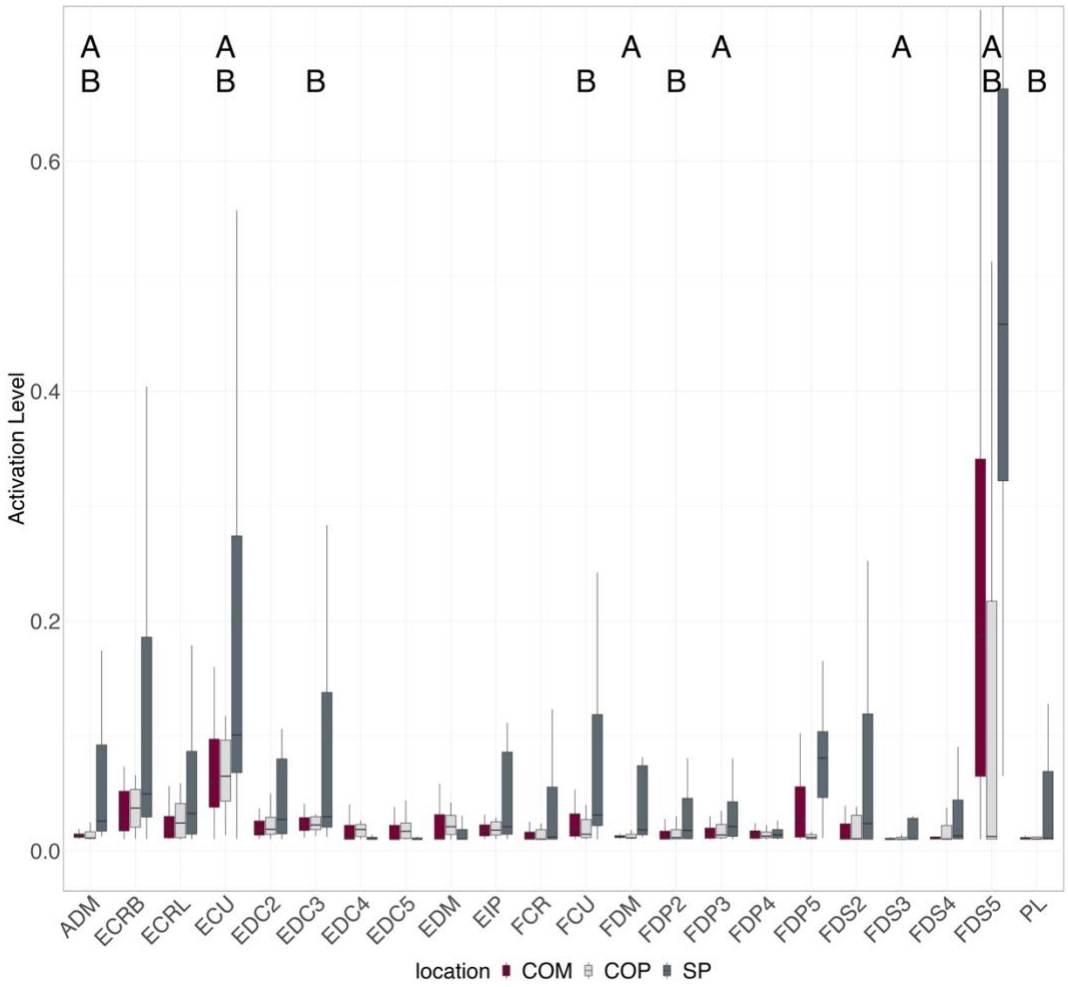

Figure 5.16. SFP5 (10 N) Box and whisker plots depicting muscle activity or forearm and finger musculature. Black horizontal lines represent the median muscle activity; box limits = upper and lower quartiles; whiskers = range. "A" = relevant difference between the COM-SP comparisons. "B" = relevant difference between the COP-SP comparison,

CHAPTER 6

DISCUSSION

The aim of this thesis was to evaluate the effect of distributed hand loads on 1) net joint moments and 2) muscle activations in the wrist and forearm during finger pressing and power gripping tasks. External loads were represented in three ways: 1) distributed across the hand applied to the centre of mass of each segment (COM), 2) distributed across the hand applied to the centre of pressure of each segment (COP), and 3) a single point force applied to the centre of mass of one segment (SP). Statistical analyses indicated practical and statistical differences between SP and COM along with SP and COP, but there was no difference between COM and COP. Thus, COM and COP are functionally similar. Essentially, COM and COP only differ in the location of the point of force application, which is limited with the small dimensions of the finger. These small differences result in typically negligible differences in model outputs (net joint moments and muscle activations), as the change in moment arm length of the external force is trivial when compared to the distribution force.

There were differences in most internal net joint moments using COM and COP compared to SP. The hypothesis that SP would have higher moments than COM and COP were partially supported. During the multiple finger presses (MFP23, MFP234, MFP2345), some digits had higher moments with COM and COP than SP. Power grips (PG20 and PG40) consistently had larger moments with COM and COP. In the pinch grip trials, some digits with higher flexion moments in COM and COP, and others with higher flexion moments in SP. Single finger presses (SFP2, SFP3, SFP4, and SFP5), had larger flexion and abduction moments in SP compared to COM and COP in all active fingers.

As a result of the differences in moments, there were differences the computed in muscle activation. The hypothesis that SP would have larger muscle activations was supported in most tasks. Wrist and digit flexors during the multi finger presses had higher activations with SP the other two models. Wrist and finger extensor activations were higher with COM and COP models in the power grip trials, yet the digit flexors had higher activations with SP. The SP model resulted in higher wrist and finger flexor activations in single finger presses. Interestingly, COM and COP had higher ECU activation during the multiple and single finger presses. This co-contraction may be due to balancing out the moments of digits with higher percentages of total force during those postures. With SP, we do not see it at the same level of activation due to the lower moments. Finger extensor activation is required during finger pressing tasks (Valero-Cuevas et al., 1998), and is typically not seen in optimization models. Using distributed loads, as in the COM and COP solutions, allowed for a co-contraction solution which is important to realistic estimations of internal forces, and subsequently the development of musculoskeletal disorders.

The MCP joint moments in the SP approach were similar to MacIntosh et al. (2014), who modeled a similar single finger press at the same force level. Similar flexion moments at the MCP, and IP joints were found in a during maximal gripping when those data were scaled proportionally to the submaximal levels of this study (Goislard De Monsabert et al., 2012). Computed finger flexor and extensor muscle activations during power grips were lower than EMG collected in a gripping study (Mogk & Keir, 2003). There are challenges in comparing computed muscle activations to surface EMG, as they are not the same (Hicks et al., 2015). Part of that, is models represent muscle compartments (e.g. FDS 2, FDS 3, FDS,4 and FDS 5) as

independent actuators. However, there can be neural and mechanical interdependencies that can lead to differences in the activations compared to empirical data (Mulla & Keir, 2023).

There are unequal contributions to force between digits during isometric tasks (Li et al., 2000; Zatsiorsky et al., 2000), which explains why some sensors had higher percentages of total force compared to others. For example, the distal phalanx of digit 2 during MFP23 had 46% $\pm$ 18% and digit 3 during MFP23 had 34% $\pm$ 15 of the total force. When compared to 50% of total force placed at the same segment with the SP approach, COM/COP second digit MCP flexion moments were larger due to the larger contribution to force from digit 2 compared to digit 3. Representing loads in this manner accounts for individual differences in load sharing between the digits and between participants when the traditional single point model did not.

Variability is prominent in the joint moments and muscle activations. One of the factors in the computation of internal forces is the magnitude of external loads placed on the bodies of interest. The moments from COM and COP have larger variability in most cases compared to SP. Results indicate some between participant standard deviations of the distributions are equal to their respective means (Table 5.1). Distributed loads account for variability in how individuals complete the same task, as each person can generate the same internal forces in a number of different ways due to the redundancy of our musculoskeletal anatomy (Mulla & Keir, 2023). Along the same lines, the variations in posture between participants during the same task result in differences in model outputs (joint moments and muscle activations). While the tasks were static and each participant was given the same instructions, finger and wrist postures differed between participants, and even within each participant's three trials, leading to the large range of moments and muscle activations. Another factor to consider is the anatomical differences between participants. The OpenSim model was anthropometrically scaled for each participant,

resulting in different internal and external moment arms. An important factor in "personalizing" models is scaling for muscle strength. Without detailed information on each muscle for each individual, this was left constant for all participants, thus, the model uses the same strength for all 23 participants.

This thesis provides insight into quantifying internal forces using distributed loads. With high numbers of injury claims to the upper extremities (Tilley et al., 2023), it is important to find ways to quantify hand forces in the workplace. As an advancement of my previous work (Chhiba et al., 2022), it shows the potential that pressure mapping can provide on quantifying hand-object interactions during workplace tasks and activities of daily living. The portable nature of the system allows it to be taken into the workplace to collect data during work tasks. The apparatus can be secured onto the worker and shape of the sensors allow for objects to be manipulated freely. The TekScan Grip System provides a novel way to quantify these forces during different hand tasks and can be used to assess the contribution of individual fingers, to evaluate changes in distributions during tasks, how pressures at the hand change with muscular fatigue, and more. Pressure mapping offers a way to quantify differences in hand loading between workers. As shown with the high variability of the pressure distributions throughout the tasks, people employ different loading strategies which in turn lead to different internal loads. This may provide insight into why some people develop musculoskeletal injuries compared to others when completing the same work tasks. Distributed loads account for individual and between task variability in external and internal loads.

The importance of implementing distributed forces is seen in the finger flexion moments in this thesis. Flexor moments in fingers with larger percentages of total force were overestimated with the single point approach (SP), and as a result, wrist and finger flexor

activations were also overestimated. Without a distributed load, these changes in loading would have not been accounted for. The information from the distributed load (higher moments, and larger co-contraction) is important to consider when assessing development of musculoskeletal disorders. The implementation of distributed loads can provide more detail into the loading that leads to workplace injuries.

Biomechanical models evolve over time. Previous finger and hand models used a single point of force application at the centre of mass of the distal phalanx for a given digit (MacIntosh & Keir, 2017; Mirakhorlo et al., 2018; Vigouroux et al., 2009), or at the distal tip of the finger (Lee et al., 2015; McFarland et al., 2023; Vigouroux et al., 2009). For example, McFarland et al. (2023) developed the model used in this thesis and simulated power grips, but only applied external forces at the proximal and intermediate phalanges with no contributions from the thumb. Similar to the results from SP in this thesis, their simulations computed muscle and grip forces higher than previous literature. Force distributions quantified in this thesis show that even during a single finger press, there are multiple points of contact, and therefore forces being exerted at different parts of the digit. While there is less emphasis on where the loads act (at the COM or COP), there is a trend of overestimating loads with the single point model when compared to the distributed load models. Researchers should consider distributing loads when applying external loads to account for the greater distribution of loads and remove the assumption that all forces at the hand act at a single point. At a minimum, implementation of a distributed forces approach using the COM provides an improved representation of hand-object interactions. A distributed load model allows better fidelity of hand loading and results in greater distribution of internal loads.

6.1 Limitations

There are some limitations to this study. First, the tasks of interest were all single-handed and static. The exploratory nature of this thesis warranted the tasks to be simple to assess the capabilities of the system before trying more complex tasks. Secondly, the size of the sensors is fixed, so a participant with smaller hands might have the sensors wrap around the lateral sides of the digit, which may register as pressures in the lateral direction during tasks. In contrast, the sensors on a larger hand may not completely cover the palmar surfaces. This was mitigated by ensuring that 90 percent of the participants' force was in the vertical direction using the force transducer. Third, the customized OpenSim ARMS model contained only musculature of the forearm and fingers, which was not strength scaled for each participant. Muscle scaling was held constant for all participants to avoid adding another source of variability of unknown consequence. Fourth, EMG was not collected to compare to model outputs due to the exploratory nature of the study and space constraints on the forearm. Finally, it was assumed that the centre of the sensor was placed at the centre of mass of the segment and during the finger press tasks, only functional pressures and forces were considered. For example, during SFP2, incidental contact of the palm, was not represented as an external force acting on the hand.

6.2 Future Directions

Looking to future work, a detailed analysis of effect sizes of variables is warranted. A series of Monte Carlo simulations can be used to vary the force, load distribution and placement, and posture during these tasks to assess the role each plays in determining joint moments and muscle activations. Strength scaling the model would also provide more insight and relevance to muscle activations simulated in this thesis. Future studies should look at a wider range of tasks

that mimic other workplace actions and activities of daily living. Bi-manual and dynamic tasks such as lifting can provide information about differences in load distribution between the two hands and how that affects internal loading. It may also offer insight to how people employ different distribution strategies within and between subjects.

6.3 Conclusion

This thesis is unique as it implements the use of a hand pressure mapping system to quantify multiple points of force application at the hands. Internal loads were calculated with a biomechanical model using distributed loads from the pressure map as external forces and compared to the traditional single point application of an external load. Findings indicate that digits with higher percentages of total force have higher moments and higher muscle activations compared to the single point model. Distributing loads can account for the unequal force contributions between fingers and co-contraction when calculating internal loads. The distributed loads applied in this thesis can be used as a stepping stone towards improving the representation of external loads in biomechanical models. A new perspective to representing external loads has been explored and further work will only improve current representations of loads, leading to more realistic models of the hands and fingers. This in turn can be used in occupational, clinical and many other settings to monitor the internal loads that contribute to the development of musculoskeletal injuries.

REFERENCES

Austin, E. F., Kearney, C. P., Chacon, P. J., Winges, S. A., Acharya, P., & Choi, J.-W. (2022). A Fabricated Force Glove That Measures Hand Forces during Activities of Daily Living. *Sensors*, *22*(4), 1330.

Barry, A. J., Murray, W. M., & Kamper, D. G. (2018). Development of a dynamic index finger and thumb model to study impairment. *Journal of Biomechanics*, *77*, 206–210.

Brook, N., Mizrahi, J., Shoham, M., & Dayan, J. (1995). A biomechanical model of index finger dynamics. *Medical Engineering & Physics*, *17*(1), 54–63.

Chhiba, R., Majoni, T. N., Paul, M. T., & Daanish, M. M. (2022, August). Evaluating the Influence of Multiple Pressure Points on the Hand and Fingers. *Poster Abstracts*. North American Congress of Biomechanics, Ottawa, ON.

Cutkosky, M. R. (1989). On grasp choice, grasp models, and the design of hands for manufacturing tasks. *IEEE Transactions on Robotics and Automation*, *5*(3), 269–279.

Ergen, H. I., & Oksuz, C. (2020). Evaluation of Load Distributions and Contact Areas in 4 Common Grip Types Used in Daily Living Activities. *The Journal of Hand Surgery*, *45*(3), 251.e1-251.e8.

Goislard De Monsabert, B., Rossi, J., Berton, É., & Vigouroux, L. (2012). Quantification of Hand and Forearm Muscle Forces during a Maximal Power Grip Task. *Medicine & Science in Sports & Exercise*, *44*(10), 1906–1916.

Hicks, J. L., Uchida, T. K., Seth, A., Rajagopal, A., & Delp, S. L. (2015). Is My Model Good Enough? Best Practices for Verification and Validation of Musculoskeletal Models and Simulations of Movement. *Journal of Biomechanical Engineering*, *137*(2), 0209051–02090524.

Holzbaur, K. R. S., Murray, W. M., & Delp, S. L. (2005). A Model of the Upper Extremity for Simulating Musculoskeletal Surgery and Analyzing Neuromuscular Control. *Annals of Biomedical Engineering*, *33*(6), 829–840.

Hung, C.-F., Chen, C.-C., Lin, S.-H., & Chung, T.-K. (2017). Finger and Palm Dynamic Pressure Monitoring for Basketball Shooting. *Journal of Sensors*, *2017*, 1–5.

Iberall, T. (1987). The nature of human prehension: Three dextrous hands in one. *Proceedings. 1987 IEEE International Conference on Robotics and Automation*, *4*, 396–401.

Keenan, K. G., & Massey, W. V. (2012). Control of Fingertip Forces in Young and Older Adults Pressing against Fixed Low- and High-Friction Surfaces. *PLOS ONE*, *7*(10), e48193.

Keir, P. J., Farias Zuniga, A., Mulla, D. M., & Somasundram, K. G. (2021). Relationships and Mechanisms Between Occupational Risk Factors and Distal Upper Extremity Disorders. *Human Factors*, *63*(1), 5–31.

Lakens, D. (2017). Equivalence Tests. *Social Psychological and Personality Science*, *8*(4), 355–362.

Lakens, D., Scheel, A. M., & Isager, P. M. (2018). Equivalence Testing for Psychological Research: A Tutorial. *Advances in Methods and Practices in Psychological Science*, *1*(2), 259–269.

Lee, J. H., Asakawa, D. S., Dennerlein, J. T., & Jindrich, D. L. (2015). Extrinsic and Intrinsic Index Finger Muscle Attachments in an OpenSim Upper-Extremity Model. *Annals of Biomedical Engineering*, *43*(4), 937–948.

Li, S., Danion, F., Latash, M. L., Li, Z.-M., & Zatsiorsky, V. M. (2000). Characteristics of finger force production during one- and two-hand tasks. *Human Movement Science*, *19*(6), 897–923.

MacIntosh, A. R., & Keir, P. J. (2017). An open-source model and solution method to predict co-contraction in the finger. *Computer Methods in Biomechanics and Biomedical Engineering*, *20*(13), 1373–1381.

Mastalerz, A., Nowak, E., Palczewska, I., & Kalka, E. (2009). Maximal Grip Force During Holding A Cylindrical Handle with Different Diameters. *Human Movement*, *10*(1).

McFarland, D. C., Binder-Markey, B. I., Nichols, J. A., Wohlman, S. J., De Bruin, M., & Murray, W. M. (2023). A Musculoskeletal Model of the Hand and Wrist Capable of Simulating Functional Tasks. *IEEE Transactions on Biomedical Engineering*, *70*(5), 1424–1435.

Mirakhorlo, M., Van Beek, N., Wesseling, M., Maas, H., Veeger, H. E. J., & Jonkers, I. (2018). A musculoskeletal model of the hand and wrist: Model definition and evaluation. *Computer Methods in Biomechanics and Biomedical Engineering*, *21*(9), 548–557.

Mühldorfer-Fodor, M., Ziegler, S., Harms, C., Neumann, J., Kundt, G., Mittlmeier, T., & Prommersberger, K. J. (2017). Load distribution of the hand during cylinder grip analyzed by Manugraphy. *Journal of Hand Therapy*, *30*(4), 529–537.

Mulla, D. M., & Keir, P. J. (2023). Neuromuscular control: From a biomechanist's perspective. *Frontiers in Sports and Active Living*, *5*, 1217009.

Napier, J. R. (1956). THE PREHENSILE MOVEMENTS OF THE HUMAN HAND. *The Journal of Bone and Joint Surgery. British Volume*, *38-B*(4), 902–913.

Netter, F. H. (2011). *Atlas of Human Anatomy, Professional Edition*. Netter Better Science.

Nichols, J. A., Bednar, M. S., Wohlman, S. J., & Murray, W. M. (2017). Connecting the wrist to the hand: A simulation study exploring changes in thumb-tip endpoint force following wrist surgery. *Journal of Biomechanics*, *58*, 97–104.

Prendergast, N., & Rauschning, W. (1995). NORMAL ANATOMY OF THE HAND AND WRIST. *Magnetic Resonance Imaging Clinics of North America*, *3*(2), 197–212.

Sanford, J., Young, C., Popa, D., Bugnariu, N., & Patterson, R. (2014). *Grip pressure measurements during activities of daily life* (D. O. Popa & M. B. J. Wijesundara, Eds.; p. 91160H).

Seo, N. J., & Armstrong, T. J. (2008). Investigation of Grip Force, Normal Force, Contact Area, Hand Size, and Handle Size for Cylindrical Handles. *Human Factors: The Journal of the Human Factors and Ergonomics Society*, *50*(5), 734–744.

Sinsel, E. W., Gloekler, D. S., Wimer, B. M., Warren, C. M., Wu, J. Z., & Buczek, F. L. (2016). Automated pressure map segmentation for quantifying phalangeal kinetics during cylindrical gripping. *Medical Engineering & Physics*, *38*(2), 72–79.

Statistics | AWCBC / ACATC. (2021, December 5). AWCBC / ACATC | Connecting Members - Advancing Knowledge / Relier Les Membres - Développer Les Connaissances. https://awcbc.org/en/statistics/

Tilley, P. M., Mulla, D. M., & Keir, P. J. (2023). Effects of sex and age on work-related upper extremity musculoskeletal disorders in Ontario, Canada. *Work*, *75*(3), 1009–1020.

Valero-Cuevas, F. J., Johanson, M. E., & Towles, J. D. (2003). Towards a realistic biomechanical model of the thumb: The choice of kinematic description may be more critical than the solution method or the variability/uncertainty of musculoskeletal parameters. *Journal of Biomechanics*, *36*(7), 1019–1030.

Valero-Cuevas, F. J., Zajac, F. E., & Burgar, C. G. (1998). Large index-fingertip forces are produced by subject-independent patterns of muscle excitation. *Journal of Biomechanics*, *8*(31), 693–703.

Veiersted, K. B., Westgaard, R. H., & Andersen, P. (1990). Pattern of muscle activity during stereotyped work and its relation to muscle pain. *International Archives of Occupational and Environmental Health*, *62*(1), 31–41.

Vigouroux, L., Domalain, M., & Berton, E. (2009). Comparison of tendon tensions estimated from two biomechanical models of the thumb. *Journal of Biomechanics*, *42*(11), 1772–1777.

Wright, R. D. (1935). A Detailed Study of Movement of the Wrist Joint. *Journal of Anatomy*, *70*(Pt 1), 137-142.1.

Zakaria, D., Robertson, J., MacDermid, J. C., Hartford, K., & Koval, J. (2002). Estimating the population at risk for Ontario Workplace Safety and Insurance Board-covered injuries or diseases. *Chronic Diseases in Canada*, *23*(1), 17–21.

Zatsiorsky, V. M., Li, Z.-M., & Latash, M. L. (2000). Enslaving effects in multi-finger force production. *Experimental Brain Research*, *131*(2), 187–195.

APPENDIX A – Supplementary Methods

Figure A1. Experimental setup. Participants sat at this table to perform the tasks of interest. They received feedback from the monitor in front of them. They were asked to match the green line (set at each specified force).

APPENDIX B – Supplementary Results Tables

Table B1. Within participant (between trials) pressure variability for each sensor for each task across all participants (expressed as percent of sum of pressure on all included sensors).

Task		MFP23	MFP234	MFP2345	PG20	PG40	SFP2	SFP3	SFP4	SFP5	Pinch
Distal Phalange	*Digit 1*	-	0.1 (0)	-	0.7	0.9	-	-	-	-	0.9
Proximal Phalange		-	-	-	0.4	0.3	-	-	-	-	0.4
Distal Phalange	*Digit 2*	4.6	4.1	2.4	2.3	2.2	4.2	-	-	-	3.7
Middle Phalange		1.9	2.2	1.0	2.3	2.9	3.3	-	-	-	3.9
Proximal Phalange		2.0	1.4	0.9	2.6	2.9	2.3	-	-	-	0.5
Distal Phalange	*Digit 3*	4.0	3.1	2.8	1.8	1.1	-	5.2	-	-	3.1
Middle Phalange		1.9	1.3	1.5	2.6	1.3	-	2.6	-	-	1.1
Proximal Phalange		1.2	1.2	2.2	1.2	1.1	-	3.9	-	-	0.7
Distal Phalange	*Digit 4*	-	2.0	1.6	1.1	1.0	-	-	6.0	-	2.3
Middle Phalange		-	2.2	1.3	2.0	1.6	-	-	5.1	-	1.5
Proximal Phalange		-	0.8	0.8	0.7	0.8	-	-	3.0	-	1.6
Distal Phalange	*Digit 5*	-	-	1.4	0.6	0.5	-	-	-	8.6	1.7
Middle Phalange		-	-	2.7	0.5	0.4	-	-	-	7.2	1.3
Proximal Phalange		-	-	0.3	0.2	0.2	-	-	-	5.7	0.2
Hypothenar Region	*Palm*	-	-	-	0.2	0.2	-	-	-	-	0.1
Metacarpal Region		-	-	-	0.3	0.3	-	-	-	-	0.1
Thenar Region		-	-	-	0.1	0.1	-	-	-	-	0.2

Table B2: Outputs of statistical analyses conducted on Inverse Dynamics results, 1) the equivalence test results (EQ) and 2) the null hypothesis significance testing results (NHST). Degrees of freedom (df) are reported next to the task. T-statistic of each test is reported. The interpretation of the equivalence test is noted. Highlighted rows indicate a relevant difference.

	SP - COM			SP -- COP		
Task	**MFP23 (df = 879)**			**MFP23 (df = 879)**		
	EQ	NHST	Interpretation	EQ	NHST	Interpretation
t-statistic	*-2.30*	*-7.50*		*-1.30*	*-6.28*	
MCP F	0.99	< 0.01	relevant diff	0.90	< 0.01	relevant diff
MCP ABD	0.99	< 0.01	relevant diff	0.90	< 0.01	relevant diff
PIP F	0.99	< 0.01	relevant diff	0.90	< 0.01	relevant diff
DIP F	0.99	< 0.01	relevant diff	0.90	< 0.01	relevant diff
Task	**MFP2345 (df = 919)**			**MFP2345 (df = 919)**		
	EQ	NHST	Interpretation	EQ	NHST	Interpretation
t-statistic	*0.31*	*-3.55*		*1.50*	*2.10*	
MCP F	0.38	< 0.01	relevant diff	0.07	0.03	indeterminate
MCP ABD	0.38	< 0.01	relevant diff	0.07	0.03	indeterminate
PIP F	0.38	< 0.01	relevant diff	0.07	0.03	indeterminate
DIP F	0.38	< 0.01	relevant diff	0.07	0.03	indeterminate
Task	**SFP3 (df = 171)**			**SFP3 (df = 171)**		
	EQ	NHST	Interpretation	EQ	NHST	Interpretation
t-statistic	*-10.00*	*-11.00*		*-10.00*	*-11.40*	
MCP F	1.00	< 0.01	relevant diff	1.00	< 0.01	relevant diff
MCP ABD	1.00	< 0.01	relevant diff	1.00	< 0.01	relevant diff
PIP F	1.00	< 0.01	relevant diff	1.00	< 0.01	relevant diff
DIP F	1.00	< 0.01	relevant diff	1.00	< 0.01	relevant diff
Task	**SFP5 (df = 175)**			**SFP5 (df = 175)**		
	EQ	NHST	Interpretation	EQ	NHST	Interpretation
t-statistic	*-7.70*	*-8.80*		*-7.30*	*-9.03*	
MCP F	1.00	< 0.01	relevant diff	1.00	< 0.01	relevant diff
MCP ABD	1.00	< 0.01	relevant diff	1.00	< 0.01	relevant diff
PIP F	1.00	< 0.01	relevant diff	1.00	< 0.01	relevant diff
DIP F	1.00	< 0.01	relevant diff	1.00	< 0.01	relevant diff
Task	**PG40 (df = 919)**			**PG40 (df = 919)**		
	EQ	NHST	Interpretation	EQ	NHST	Interpretation

t-statistic	*19.16*	*20.27*		*18.69*	*19.75*	
MCP F	1.00	< 0.01	relevant diff	1.00	< 0.01	relevant diff
MCP ABD	1.00	< 0.01	relevant diff	1.00	< 0.01	relevant diff
PIP F	1.00	< 0.01	relevant diff	1.00	< 0.01	relevant diff
DIP F	1.00	< 0.01	relevant diff	1.00	< 0.01	relevant diff
Task	**MFP234 (df = 939)**			**MFP234(df = 939)**		
	EQ	NHST	Interpretation	EQ	NHST	Interpretation
t-statistic	*-1.50*	*-5.50*		*-0.35*	*-4.63*	
MCP F	0.93	< 0.01	relevant diff	0.64	< 0.01	relevant diff
MCP ABD	0.93	< 0.01	relevant diff	0.64	< 0.01	relevant diff
PIP F	0.93	< 0.01	relevant diff	0.64	< 0.01	relevant diff
DIP F	0.93	< 0.01	relevant diff	0.64	< 0.01	relevant diff
Task	**SFP2 (df = 167)**			**SFP2(df = 171)**		
	EQ	NHST	Interpretation	EQ	NHST	Interpretation
t-statistic	*-15.00*	*-16.00*		*-13.00*	*-15.00*	
MCP F	1.00	< 0.01	relevant diff	1.00	< 0.01	relevant diff
MCP ABD	1.00	< 0.01	relevant diff	1.00	< 0.01	relevant diff
PIP F	1.00	< 0.01	relevant diff	1.00	< 0.01	relevant diff
DIP F	1.00	< 0.01	relevant diff	1.00	< 0.01	relevant diff
Task	**SFP4 (df = 171)**			**SFP4 (df = 171)**		
	EQ	NHST	Interpretation	EQ	NHST*	Interpretation
t-statistic	*-11.00*	*-12.00*		*-11.00*	*-12.22*	
MCP F	1.00	< 0.01	relevant diff	1.00	< 0.01	relevant diff
MCP ABD	1.00	< 0.01	relevant diff	1.00	< 0.01	relevant diff
PIP F	1.00	< 0.01	relevant diff	1.00	< 0.01	relevant diff
DIP F	1.00	< 0.01	relevant diff	1.00	< 0.01	relevant diff
Task	**PG20 (df = 899)**			**PG20 (df = 919)**		
	EQ	NHST	Interpretation	EQ	NHST	Interpretation
t-statistic	*16.95*	*19.18*		*16.39*	*18.53*	
MCP F	1.00	< 0.01	relevant diff	1.00	< 0.01	relevant diff
MCP ABD	1.00	< 0.01	relevant diff	1.00	< 0.01	relevant diff
PIP F	1.00	< 0.01	relevant diff	1.00	< 0.01	relevant diff
DIP F	1.00	< 0.01	relevant diff	1.00	< 0.01	relevant diff
Task	**Pinch (df = 675)**			**Pinch (df = 679)**		
	EQ	NHST	Interpretation	EQ	NHST	Interpretation

t-statistic	*1.5*	*3.1*		*-0.6*	*-2.2*	
MCP F	0.93	< 0.01	relevant diff	0.72	0.03	indeterminate
MCP ABD	0.93	< 0.01	relevant diff	0.72	0.03	indeterminate
PIP F	0.93	< 0.01	relevant diff	0.72	0.03	indeterminate
DIP F	0.93	< 0.01	relevant diff	0.72	0.03	indeterminate

Table B3: Outputs of statistical analyses conducted on muscle activations, 1) the equivalence test results (EQ) and 2) the null hypothesis significance testing results (NHST). Degrees of freedom (df) are reported next to the task. T-statistic of each test is reported. The interpretation of the equivalence test is noted. Highlighted rows indicate a relevant difference.

	SP- COM					SP-COP				
Task	**MFP23**					**MFP23**				
	EQ		NHST		Interpretation	EQ		NHST		Interpretation
	t-statistic (df)	p-value	t-statistic (df)	p-value		t-statistic (df)	p-value	t-statistic (df)	p-value	
ECRL	t(43) = -1.95	= 0.029	t(43) = 1.268	= 0.212	equivalent	t(43) = -33.8	< 0.001	t(43) = 1.792	= 0.08	equivalent
ECRB	t(43) = -9.67	< 0.001	t(43) = 0.159	= 0.874	equivalent	t(43) = -7.62	< 0.001	t(43) = 1.676	= 0.101	equivalent
ECU	t(43) = -5.59	< 0.001	t(43) = 0.669	= 0.507	equivalent	t(43) = -1.05	= 0.149	t(43) = 5.994	< 0.001	relevant diff
FCR	t(43) = 7.413	< 0.001	t(43) = -1.62	= 0.113	equivalent	t(43) = 18.87	< 0.001	t(43) = -0.89	= 0.378	equivalent
FCU	t(43) = -4.99	< 0.001	t(43) = 0.094	= 0.925	equivalent	t(43) = 10.206	< 0.001	t(43) = -2.56	= 0.014	equivalent
PL	t(43) = 17.894	< 0.001	t(43) = -1.52	= 0.136	equivalent	t(43) = 19.387	< 0.001	t(43) = -1.06	= 0.297	equivalent
FDS5	t(43) = 14.468	< 0.001	t(43) = -1.35	= 0.186	equivalent	t(43) = 12.043	< 0.001	t(43) = -0.931	= 0.357	equivalent
FDS4	t(43) = 10.529	< 0.001	t(43) = -1.05	= 0.301	equivalent	t(43) = 20.225	< 0.001	t(43) = -0.81	= 0.422	equivalent
FDS3	t(43) = -1.9	= 0.968	t(43) = -5.8	< 0.001	relevant diff	t(43) = -3.08	= 0.998	t(43) = -7.68	< 0.001	relevant diff
FDS2	t(43) = -0.839	= 0.797	t(43) = -2.64	= 0.011	equivalent	t(43) = -3.97	= 1	t(43) = -6.62	< 0.001	relevant diff
FDP5	t(43) = 18.249	< 0.001	t(43) = -2.27	= 0.028	equivalent	t(43) = 25.493	< 0.001	t(43) = -3.26	= 0.002	trivial diff
FDP4	t(43) = 9.548	< 0.001	t(43) = -2.32	= 0.025	equivalent	t(43) = 17.043	< 0.001	t(43) = -3.6	< 0.001	trivial diff
FDP2	t(43) = -4.13	= 1	t(43) = -8.21	< 0.001	relevant diff	t(43) = -8.27	= 1	t(43) = -12.8	< 0.001	relevant diff
FDP2	t(43) = -0.924	= 0.82	t(43) = -3.52	= 0.001	relevant diff	t(43) = -4.7	= 1	t(43) = -7.04	< 0.001	relevant diff
EDC5	t(43) = 11.612	< 0.001	t(43) = -0.892	= 0.377	equivalent	t(43) = -39.7	< 0.001	t(43) = 1.087	= 0.283	equivalent
EDC4	t(43) = 10.405	< 0.001	t(43) = -0.146	= 0.885	equivalent	t(43) = -9.78	< 0.001	t(43) = 1.525	= 0.135	equivalent
EDC3	t(43) = -7.56	< 0.001	t(43) = 1.539	= 0.131	equivalent	t(43) = -5.06	< 0.001	t(43) = 5.302	< 0.001	equivalent
EDC2	t(43) = -16	< 0.001	t(43) = 0.339	= 0.736	equivalent	t(43) = -8.14	< 0.001	t(43) = 3.042	= 0.004	equivalent
EDM	t(43) = -10.8	< 0.001	t(43) = 0.621	= 0.538	equivalent	t(43) = -22.9	< 0.001	t(43) = 6.682	< 0.001	trivial diff
EIP	t(43) = -12.1	< 0.001	t(43) = 0.4	= 0.691	equivalent	t(43) = -9.96	< 0.001	t(43) = 3.009	= 0.004	equivalent
ADM	t(43) = 20.942	< 0.001	t(43) = -0.764	= 0.449	equivalent	t(43) = -25.5	< 0.001	t(43) = 0.031	= 0.976	equivalent
FDM	t(43) = 19.94	< 0.001	t(43) = -1.15	= 0.258	equivalent	t(43) = 21.17	< 0.001	t(43) = -0.116	= 0.908	equivalent
Task	**MFP234**					**MFP234**				
	EQ		NHST		Interpretation	EQ		NHST		Interpretation
	t-statistic (df)	p-value	t-statistic (df)	p-value		t-statistic (df)	p-value	t-statistic (df)	p-value	
ECRL	t(46) = -1	= 0.16	t(46) = 1.782	= 0.081	indeterminate	t(46) = -3.9	< 0.001	t(46) = 0.008	= 0.994	equivalent
ECRB	t(46) = -6.92	< 0.001	t(46) = 0.673	= 0.504	equivalent	t(46) = -2.77	= 0.004	t(46) = 0.087	= 0.931	indeterminate

ECU	t(46) = -3.51	< 0.001	t(46) = 0.863	= 0.393	equivalent	t(46) = -2.04	= 0.024	t(46) = 3.75	< 0.001	relevant diff
FCR	t(46) = -3.34	< 0.001	t(46) = 1.139	= 0.26	equivalent	t(46) = 2.63	= 0.006	t(46) = -0.358	= 0.722	indeterminate
FCU	t(46) = -2.41	= 0.01	t(46) = 1.382	= 0.174	indeterminate	t(46) = 7.966	< 0.001	t(46) = -0.774	= 0.443	equivalent
PL	t(46) = 7.134	< 0.001	t(46) = -0.265	= 0.792	equivalent	t(46) = 2.146	= 0.019	t(46) = -1.04	= 0.304	indeterminate
FDS 5	t(46) = -3.86	= 1	t(46) = -6.43	< 0.001	relevant diff	t(46) = -6.24	= 1	t(46) = -8.28	< 0.001	relevant diff
FDS 4	t(46) = -1.74	= 0.955	t(46) = -5.44	< 0.001	trivial diff	t(46) = -3.07	= 0.998	t(46) = -7.86	< 0.001	relevant diff
FDS 3	t(46) = 2.368	= 0.011	t(46) = -1.04	= 0.303	indeterminate	t(46) = -0.881	= 0.808	t(46) = -4.19	< 0.001	relevant diff
FDS 2	t(46) = 0.604	= 0.275	t(46) = -1.26	= 0.215	indeterminate	t(46) = -3.05	= 0.998	t(46) = -5.58	< 0.001	relevant diff
FDP 5	t(46) = -9.45	< 0.001	t(46) = 0.877	= 0.385	equivalent	t(46) = 8.626	< 0.001	t(46) = -1.88	= 0.067	indeterminate
FDP 4	t(46) = -6.22	= 1	t(46) = -8.55	< 0.001	relevant diff	t(46) = -9.49	= 1	t(46) = -11.8	< 0.001	relevant diff
FDP 2	t(46) = -0.00953	= 0.504	t(46) = -3.49	= 0.001	relevant diff	t(46) = -6.21	= 1	t(46) = -10.6	< 0.001	relevant diff
FDP 2	t(46) = -0.424	= 0.663	t(46) = -3.05	= 0.004	indeterminate	t(46) = -3.67	= 1	t(46) = -6.16	< 0.001	relevant diff
EDC 5	t(46) = -3.67	< 0.001	t(46) = 1.172	= 0.247	equivalent	t(46) = -3.65	< 0.001	t(46) = 1.654	= 0.105	equivalent
EDC 4	t(46) = -4.78	< 0.001	t(46) = 1.475	= 0.147	equivalent	t(46) = -1.32	= 0.096	t(46) = 1.81	= 0.077	indeterminate
EDC 3	t(46) = -7.31	< 0.001	t(46) = 1.03	= 0.308	equivalent	t(46) = -2.35	= 0.012	t(46) = 0.931	= 0.356	indeterminate
EDC 2	t(46) = -12.6	< 0.001	t(46) = 0.404	= 0.688	equivalent	t(46) = -3.06	= 0.002	t(46) = 0.218	= 0.828	equivalent
EDM	t(46) = -5.88	< 0.001	t(46) = 1.748	= 0.087	equivalent	t(46) = -11.4	< 0.001	t(46) = 2.32	= 0.025	equivalent
EIP	t(46) = -8.99	< 0.001	t(46) = 0.032	= 0.975	equivalent	t(46) = 2.832	= 0.003	t(46) = -0.121	= 0.904	indeterminate
ADM	t(46) = -6.89	< 0.001	t(46) = 0.399	= 0.692	equivalent	t(46) = -6.69	< 0.001	t(46) = 0.918	= 0.363	equivalent
FDM	t(46) = 9.508	< 0.001	t(46) = -0.242	= 0.81	equivalent	t(46) = 26.218	< 0.001	t(46) = -0.0614	= 0.951	equivalent

Task	**MFP2345**					**MFP2345**				
	EQ		NHST		Interpretation	EQ		NHST		Interpretation
	t-statistic (df)	p-value	t-statistic (df)	p-value		t-statistic (df)	p-value	t-statistic (df)	p-value	
ECRL	t(45) = -1.86	= 0.035	t(45) = 0.337	= 0.738	indeterminate	t(45) = 2.495	= 0.008	t(45) = -0.132	= 0.896	indeterminate
ECRB	t(45) = -0.453	= 0.674	t(45) = -1.96	= 0.056	indeterminate	t(45) = 0.249	= 0.402	t(45) = -1.28	= 0.208	indeterminate
ECU	t(45) = -0.917	= 0.818	t(45) = -2.11	= 0.041	indeterminate	t(45) = 0.001	= 0.499	t(45) = -1.59	= 0.119	indeterminate
FCR	t(45) = 2.027	= 0.024	t(45) = -0.418	= 0.678	indeterminate	t(45) = 4.397	< 0.001	t(45) = -0.625	= 0.535	equivalent
FCU	t(45) = 2.828	= 0.003	t(45) = -0.339	= 0.736	indeterminate	t(45) = 1.609	= 0.057	t(45) = -2.38	= 0.022	indeterminate
PL	t(45) = 1.012	= 0.158	t(45) = -1.03	= 0.309	indeterminate	t(45) = 0.848	= 0.2	t(45) = -1.58	= 0.121	indeterminate
FDS 5	t(45) = -3.06	= 0.998	t(45) = -3.52	= 0.001	relevant diff	t(45) = -8.44	= 1	t(45) = -9.26	< 0.001	relevant diff
FDS 4	t(45) = -1.72	= 0.954	t(45) = -2.42	= 0.02	indeterminate	t(45) = -2.08	= 0.978	t(45) = -3.03	= 0.004	indeterminate
FDS 3	t(45) = 0.904	= 0.185	t(45) = -1.03	= 0.308	indeterminate	t(45) = 0.233	= 0.409	t(45) = -3.2	= 0.003	indeterminate
FDS 2	t(45) = -1.21	= 0.884	t(45) = -2.91	= 0.006	indeterminate	t(45) = -1.88	= 0.967	t(45) = -3.98	< 0.001	relevant diff
FDP 5	t(45) = -1.05	= 0.849	t(45) = -4.39	< 0.001	relevant diff	t(45) = -4.52	= 1	t(45) = -8.7	< 0.001	relevant diff

FDP 4	t(45) = -4.16	= 1	t(45) = -8.24	< 0.001	relevant diff	t(45) = -3.48	= 0.999	t(45) = -5.61	< 0.001	relevant diff
FDP 2	t(45) = -0.735	= 0.767	t(45) = -3.48	= 0.001	relevant diff	t(45) = -5.95	= 1	t(45) = -9.78	< 0.001	relevant diff
FDP 2	t(45) = 0.396	= 0.347	t(45) = -1.6	= 0.116	indeterminate	t(45) = -2.07	= 0.978	t(45) = -4.56	< 0.001	relevant diff
EDC 5	t(45) = -23.6	< 0.001	t(45) = 0.527	= 0.601	equivalent	t(45) = -4.48	< 0.001	t(45) = 1.992	= 0.052	equivalent
EDC 4	t(45) = -8.66	< 0.001	t(45) = 0.522	= 0.605	equivalent	t(45) = -3.18	= 0.001	t(45) = 2.726	= 0.009	equivalent
EDC 3	t(45) = -0.477	= 0.682	t(45) = -1.57	= 0.124	indeterminate	t(45) = -0.265	= 0.604	t(45) = -1.39	= 0.171	indeterminate
EDC 2	t(45) = -0.443	= 0.67	t(45) = -1.97	= 0.055	indeterminate	t(45) = 0.313	= 0.378	t(45) = -1.18	= 0.242	indeterminate
EDM	t(45) = -4.58	< 0.001	t(45) = 2.112	= 0.04	equivalent	t(45) = -2	= 0.026	t(45) = 2.542	= 0.015	indeterminate
EIP	t(45) = -0.427	= 0.664	t(45) = -1.95	= 0.058	indeterminate	t(45) = 0.084	= 0.467	t(45) = -1.4	= 0.169	indeterminate
ADM	t(45) = -0.368	= 0.643	t(45) = -2.33	= 0.024	indeterminate	t(45) = -0.616	= 0.73	t(45) = -2.66	= 0.011	indeterminate
FDM	t(45) = -0.269	= 0.605	t(45) = -2.12	= 0.04	indeterminate	t(45) = -0.375	= 0.645	t(45) = -2.29	= 0.027	indeterminate

Task	**SFP2**					**SFP2**				
	EQ		NHST		Interpretation	EQ		NHST		Interpretation
	t-statistic (df)	p-value	t-statistic (df)	p-value		t-statistic (df)	p-value	t-statistic (df)	p-value	
ECRL	t(42) = -1.55	= 0.065	t(42) = 1.577	= 0.122	indeterminate	t(42) = -11.8	< 0.001	t(42) = 1.758	= 0.086	equivalent
ECRB	t(42) = -8.64	< 0.001	t(42) = 0.764	= 0.449	equivalent	t(42) = -5.56	< 0.001	t(42) = 1.746	= 0.088	equivalent
ECU	t(42) = -4.62	< 0.001	t(42) = 2.784	= 0.008	equivalent	t(42) = -0.169	= 0.433	t(42) = 6.832	< 0.001	relevant diff
FCR	t(42) = 12.627	< 0.001	t(42) = -3.27	= 0.002	equivalent	t(42) = 34.068	< 0.001	t(42) = -4.14	< 0.001	trivial diff
FCU	t(42) = -4.27	< 0.001	t(42) = 0.909	= 0.368	equivalent	t(42) = 10.816	< 0.001	t(42) = -0.442	= 0.661	equivalent
PL	t(42) = 10.929	< 0.001	t(42) = -2.41	= 0.02	equivalent	t(42) = 13.816	< 0.001	t(42) = -2.6	= 0.013	equivalent
FDS 5	t(42) = -13.7	< 0.001	t(42) = 0.22	= 0.827	equivalent	t(42) = -43.8	< 0.001	t(42) = 0.268	= 0.79	equivalent
FDS 4	t(42) = 20.266	< 0.001	t(42) = -0.0905	= 0.928	equivalent	t(42) = -35.2	< 0.001	t(42) = 0.134	= 0.894	equivalent
FDS 3	t(42) = 53.116	< 0.001	t(42) = -1.83	= 0.074	equivalent	t(42) = -82.9	< 0.001	t(42) = 0.198	= 0.844	equivalent
FDS 2	t(42) = -4.77	= 1	t(42) = -6.31	< 0.001	relevant diff	t(42) = -7.9	= 1	t(42) = -10.3	< 0.001	relevant diff
FDP 5	t(42) = 24.033	< 0.001	t(42) = -3.33	= 0.002	trivial diff	t(42) = 19.544	< 0.001	t(42) = -1.17	= 0.248	equivalent
FDP 4	t(42) = 14.789	< 0.001	t(42) = -0.969	= 0.338	equivalent	t(42) = 15.333	< 0.001	t(42) = -0.368	= 0.715	equivalent
FDP 2	t(42) = 29.586	< 0.001	t(42) = -1.51	= 0.139	equivalent	t(42) = 30.453	< 0.001	t(42) = -1.46	= 0.152	equivalent
FDP 2	t(42) = -4.06	= 1	t(42) = -6.08	< 0.001	relevant diff	t(42) = -6.6	= 1	t(42) = -8.67	< 0.001	relevant diff
EDC 5	t(42) = -52.5	< 0.001	t(42) = 1.832	= 0.074	equivalent	t(42) = 21.628	< 0.001	t(42) = -0.397	= 0.694	equivalent
EDC 4	t(42) = -18.7	< 0.001	t(42) = 3.757	< 0.001	trivial diff	t(42) = -23.1	< 0.001	t(42) = 6.317	< 0.001	trivial diff
EDC 3	t(42) = -8.61	< 0.001	t(42) = 1.258	= 0.215	equivalent	t(42) = -4.28	< 0.001	t(42) = 1.704	= 0.096	equivalent
EDC 2	t(42) = -18.3	< 0.001	t(42) = 2.115	= 0.04	equivalent	t(42) = -9.34	< 0.001	t(42) = 2.813	= 0.007	equivalent
EDM	t(42) = -23.5	< 0.001	t(42) = 2.626	= 0.012	equivalent	t(42) = -7.24	< 0.001	t(42) = 1.774	= 0.083	equivalent
EIP	t(42) = -12.5	< 0.001	t(42) = 1.624	= 0.112	equivalent	t(42) = -7.6	< 0.001	t(42) = 2.408	= 0.021	equivalent

ADM	t(42) = 8.179	< 0.001	t(42) = -0.547	= 0.587	equivalent	t(42) = -9.7	< 0.001	t(42) = 0.111	= 0.912	equivalent
FDM	t(42) = 7.374	< 0.001	t(42) = -0.574	= 0.569	equivalent	t(42) = 9.012	< 0.001	t(42) = -0.861	= 0.394	equivalent

Task	**SFP3**					**SFP3**				
	EQ		NHST		Interpretation	EQ		NHST		Interpretation
	t-statistic (df)	p-value	t-statistic (df)	p-value		t-statistic (df)	p-value	t-statistic (df)	p-value	
ECRL	t(43) = -3.18	= 0.001	t(43) = 1.277	= 0.209	equivalent	t(43) = -8.42	< 0.001	t(43) = 2.137	= 0.038	equivalent
ECRB	t(43) = -9.71	< 0.001	t(43) = 2.084	= 0.043	equivalent	t(43) = -5.35	< 0.001	t(43) = 2.941	= 0.005	equivalent
ECU	t(43) = -6.2	< 0.001	t(43) = 2.247	= 0.03	equivalent	t(43) = -2.1	= 0.021	t(43) = 3.781	< 0.001	relevant diff
FCR	t(43) = -6.03	< 0.001	t(43) = 1.16	= 0.252	equivalent	t(43) = -5.48	< 0.001	t(43) = 1.04	= 0.304	equivalent
FCU	t(43) = 6.37	< 0.001	t(43) = -1.32	= 0.193	equivalent	t(43) = 3.97	< 0.001	t(43) = -4.04	< 0.001	trivial diff
PL	t(43) = -33.8	< 0.001	t(43) = 0.311	= 0.757	equivalent	t(43) = 14.586	< 0.001	t(43) = -1.75	= 0.088	equivalent
FDS5	t(43) = 2.912	= 0.003	t(43) = -1.27	= 0.21	indeterminate	t(43) = 3.41	< 0.001	t(43) = -0.943	= 0.351	equivalent
FDS4	t(43) = 6.834	< 0.001	t(43) = -0.666	= 0.509	equivalent	t(43) = 6.609	< 0.001	t(43) = -0.578	= 0.566	equivalent
FDS3	t(43) = -4.56	= 1	t(43) = -8.31	< 0.001	relevant diff	t(43) = -7.86	= 1	t(43) = -11.7	< 0.001	relevant diff
FDS2	t(43) = -11	< 0.001	t(43) = 0.71	= 0.481	equivalent	t(43) = -7.2	< 0.001	t(43) = 0.931	= 0.357	equivalent
FDP5	t(43) = 14.527	< 0.001	t(43) = -0.458	= 0.649	equivalent	t(43) = 18.853	< 0.001	t(43) = -1.32	= 0.192	equivalent
FDP4	t(43) = 3.96	< 0.001	t(43) = -0.783	= 0.438	equivalent	t(43) = 3.29	= 0.001	t(43) = -1.61	= 0.114	equivalent
FDP2	t(43) = -4.1	= 1	t(43) = -7.39	< 0.001	relevant diff	t(43) = -8.81	= 1	t(43) = -12.2	< 0.001	relevant diff
FDP2	t(43) = 5.733	< 0.001	t(43) = -0.965	= 0.34	equivalent	t(43) = 25.993	< 0.001	t(43) = -0.751	= 0.457	equivalent
EDC5	t(43) = 9.483	< 0.001	t(43) = -0.861	= 0.394	equivalent	t(43) = 10.635	< 0.001	t(43) = -0.489	= 0.627	equivalent
EDC4	t(43) = -5.57	< 0.001	t(43) = 2.215	= 0.032	equivalent	t(43) = -6.33	< 0.001	t(43) = 0.636	= 0.528	equivalent
EDC3	t(43) = -4.35	< 0.001	t(43) = 3.62	< 0.001	trivial diff	t(43) = -1.89	= 0.033	t(43) = 6.065	< 0.001	relevant diff
EDC2	t(43) = -15.9	< 0.001	t(43) = 2.167	= 0.036	equivalent	t(43) = -15.5	< 0.001	t(43) = 2.856	= 0.007	equivalent
EDM	t(43) = -10.6	< 0.001	t(43) = 1.106	= 0.275	equivalent	t(43) = -12.5	< 0.001	t(43) = 0.867	= 0.391	equivalent
EIP	t(43) = -13	< 0.001	t(43) = 2.709	= 0.01	equivalent	t(43) = -13.9	< 0.001	t(43) = 1.901	= 0.064	equivalent
ADM	t(43) = 5.253	< 0.001	t(43) = -1.37	= 0.178	equivalent	t(43) = -15.4	< 0.001	t(43) = 0.313	= 0.756	equivalent
FDM	t(43) = 6.424	< 0.001	t(43) = -0.76	= 0.451	equivalent	t(43) = 9.483	< 0.001	t(43) = -0.611	= 0.545	equivalent

Task	**SFP4**					**SFP4**				
	EQ		NHST		Interpretation	EQ		NHST		Interpretation
	t-statistic (df)	p-value	t-statistic (df)	p-value		t-statistic (df)	p-value	t-statistic (df)	p-value	
ECRL	t(42) = -2.46	= 0.009	t(42) = 1.232	= 0.225	indeterminate	t(42) = -6.83	< 0.001	t(42) = 0.931	= 0.357	equivalent
ECRB	t(42) = -8.09	< 0.001	t(42) = 0.856	= 0.397	equivalent	t(42) = -4.59	< 0.001	t(42) = 1.821	= 0.076	equivalent
ECU	t(42) = 10.877	< 0.001	t(42) = -0.538	= 0.593	equivalent	t(42) = 6.904	< 0.001	t(42) = -0.0945	= 0.925	equivalent
FCR	t(42) = 13.957	< 0.001	t(42) = -0.212	= 0.833	equivalent	t(42) = 14.061	< 0.001	t(42) = -1.49	= 0.143	equivalent

FCU	t(42) = -6.71	< 0.001	t(42) = 0.127	= 0.9	equivalent	t(42) = 10.228	< 0.001	t(42) = -2.75	= 0.009	equivalent
PL	t(42) = 21.928	< 0.001	t(42) = -1.16	= 0.254	equivalent	t(42) = -24.3	< 0.001	t(42) = 0.503	= 0.618	equivalent
FDS 5	t(42) = -7.56	= 1	t(42) = -9.35	< 0.001	relevant diff	t(42) = -8.59	= 1	t(42) = -10	< 0.001	relevant diff
FDS 4	t(42) = -6.88	= 1	t(42) = -9.5	< 0.001	relevant diff	t(42) = -8.81	= 1	t(42) = -11.7	< 0.001	relevant diff
FDS 3	t(42) = 13.06	< 0.001	t(42) = -1.33	= 0.192	equivalent	t(42) = 14.793	< 0.001	t(42) = -1.59	= 0.12	equivalent
FDS 2	t(42) = 13.676	< 0.001	t(42) = -1.56	= 0.127	equivalent	t(42) = 77.856	< 0.001	t(42) = -1.73	= 0.091	equivalent
FDP 5	t(42) = 6.701	< 0.001	t(42) = -1.93	= 0.061	equivalent	t(42) = 9.146	< 0.001	t(42) = -2.15	= 0.037	equivalent
FDP 4	t(42) = -8.2	= 1	t(42) = -10.2	< 0.001	relevant diff	t(42) = -11.2	= 1	t(42) = -13.1	< 0.001	relevant diff
FDP 2	t(42) = 12.738	< 0.001	t(42) = -1.17	= 0.249	equivalent	t(42) = 14.672	< 0.001	t(42) = -0.855	= 0.397	equivalent
FDP 2	t(42) = 14.991	< 0.001	t(42) = -0.813	= 0.421	equivalent	t(42) = 14.098	< 0.001	t(42) = -0.933	= 0.356	equivalent
EDC 5	t(42) = -9.16	< 0.001	t(42) = 0.384	= 0.703	equivalent	t(42) = -4.96	< 0.001	t(42) = 0.654	= 0.517	equivalent
EDC 4	t(42) = -5.1	< 0.001	t(42) = 2.978	= 0.005	equivalent	t(42) = -1.54	= 0.066	t(42) = 2.832	= 0.007	indeterminate
EDC 3	t(42) = -12.8	< 0.001	t(42) = 1.494	= 0.143	equivalent	t(42) = -7.19	< 0.001	t(42) = 2.978	= 0.005	equivalent
EDC 2	t(42) = -12.9	< 0.001	t(42) = 0.069	= 0.945	equivalent	t(42) = -12.3	< 0.001	t(42) = 1.812	= 0.077	equivalent
EDM	t(42) = -6.51	< 0.001	t(42) = 0.89	= 0.379	equivalent	t(42) = -8.3	< 0.001	t(42) = 2.149	= 0.037	equivalent
EIP	t(42) = -10.8	< 0.001	t(42) = 0.459	= 0.648	equivalent	t(42) = -17.9	< 0.001	t(42) = 1.004	= 0.321	equivalent
ADM	t(42) = 19.136	< 0.001	t(42) = -1.01	= 0.317	equivalent	t(42) = -11.3	< 0.001	t(42) = 0.442	= 0.661	equivalent
FDM	t(42) = 9.591	< 0.001	t(42) = -1.14	= 0.26	equivalent	t(42) = -10.5	< 0.001	t(42) = 0.14	= 0.889	equivalent

Task	**SFP5**					**SFP5**				
	EQ		NHST		Interpretation	EQ		NHST		Interpretation
	t-statistic (df)	p-value	t-statistic (df)	p-value		t-statistic (df)	p-value	t-statistic (df)	p-value	
ECRL	t(43) = -0.418	= 0.661	t(43) = -2.29	= 0.027	indeterminate	t(43) = -0.207	= 0.582	t(43) = -2.65	= 0.011	indeterminate
ECRB	t(43) = -1.83	= 0.963	t(43) = -2.64	= 0.012	indeterminate	t(43) = -1.93	= 0.97	t(43) = -2.99	= 0.005	indeterminate
ECU	t(43) = -3.09	= 0.998	t(43) = -3.86	< 0.001	relevant diff	t(43) = -3.06	= 0.998	t(43) = -4.04	< 0.001	relevant diff
FCR	t(43) = -0.0696	= 0.528	t(43) = -2.9	= 0.006	indeterminate	t(43) = 0.283	= 0.389	t(43) = -2.64	= 0.012	indeterminate
FCU	t(43) = -1.11	= 0.863	t(43) = -2.94	= 0.005	indeterminate	t(43) = -2.12	= 0.98	t(43) = -4.4	< 0.001	relevant diff
PL	t(43) = -1.7	= 0.952	t(43) = -3.2	= 0.003	indeterminate	t(43) = -1.76	= 0.957	t(43) = -3.4	= 0.001	relevant diff
FDS 5	t(43) = -5.68	= 1	t(43) = -6.07	< 0.001	relevant diff	t(43) = -10.3	= 1	t(43) = -10.9	< 0.001	relevant diff
FDS 4	t(43) = -1.67	= 0.949	t(43) = -2.78	= 0.008	indeterminate	t(43) = -1.02	= 0.844	t(43) = -2.39	= 0.021	indeterminate
FDS 3	t(43) = 0.267	= 0.395	t(43) = -3.35	= 0.002	relevant diff	t(43) = 0.615	= 0.271	t(43) = -3.17	= 0.003	indeterminate
FDS 2	t(43) = -0.962	= 0.829	t(43) = -3.02	= 0.004	indeterminate	t(43) = -0.85	= 0.8	t(43) = -3.44	= 0.001	relevant diff
FDP 5	t(43) = -2.92	= 0.997	t(43) = -5.78	< 0.001	relevant diff	t(43) = -5.1	= 1	t(43) = -7.5	< 0.001	relevant diff
FDP 4	t(43) = 1.539	= 0.066	t(43) = -1.7	= 0.096	indeterminate	t(43) = 1.921	= 0.031	t(43) = -1.74	= 0.089	indeterminate
FDP 2	t(43) = -0.667	= 0.746	t(43) = -3.33	= 0.002	relevant diff	t(43) = -0.401	= 0.655	t(43) = -3.3	= 0.002	indeterminate
FDP 2	t(43) = -1.58	= 0.939	t(43) = -2.98	= 0.005	indeterminate	t(43) = -1.16	= 0.874	t(43) = -3.55	< 0.001	relevant diff
EDC 5	t(43) = -4.4	< 0.001	t(43) = 1.488	= 0.144	equivalent	t(43) = -2.56	= 0.007	t(43) = 2.918	= 0.006	indeterminate

EDC 4	t(43) = -5.7	< 0.001	t(43) = 0.18	= 0.858	equivalent	t(43) = -3.32	< 0.001	t(43) = 1.687	= 0.099	equivalent
EDC 3	t(43) = -2.5	= 0.992	t(43) = -3.17	= 0.003	indeterminate	t(43) = -2.5	= 0.992	t(43) = -3.3	= 0.002	relevant diff
EDC 2	t(43) = -2.29	= 0.987	t(43) = -3.05	= 0.004	indeterminate	t(43) = -2.17	= 0.982	t(43) = -3.03	= 0.004	indeterminate
EDM	t(43) = -2.3	= 0.013	t(43) = 2.504	= 0.016	indeterminate	t(43) = -0.855	= 0.199	t(43) = 3.02	= 0.004	indeterminate
EIP	t(43) = -2.29	= 0.987	t(43) = -3.04	= 0.004	indeterminate	t(43) = -2.27	= 0.986	t(43) = -3.14	= 0.003	indeterminate
ADM	t(43) = -2.86	= 0.997	t(43) = -3.99	< 0.001	relevant diff	t(43) = -2.45	= 0.991	t(43) = -3.76	< 0.001	relevant diff
FDM	t(43) = -2.49	= 0.992	t(43) = -3.53	= 0.001	relevant diff	t(43) = -2.29	= 0.987	t(43) = -3.51	= 0.001	indeterminate

Task	**PG20**					**PG20**				
	EQ		NHST		Interpretation	EQ		NHST		Interpretation
	t-statistic (df)	p-value	t-statistic (df)	p-value		t-statistic (df)	p-value	t-statistic (df)	p-value	
ECRL	t(45) = 6.808	= 1	t(45) = 7.954	< 0.001	relevant diff	t(45) = 5.164	= 1	t(45) = 6.302	< 0.001	relevant diff
ECRB	t(45) = 7.867	= 1	t(45) = 8.604	< 0.001	relevant diff	t(45) = 7.439	= 1	t(45) = 8.412	< 0.001	relevant diff
ECU	t(45) = 3.317	= 0.999	t(45) = 4.714	< 0.001	relevant diff	t(45) = 3.45	= 0.999	t(45) = 4.534	< 0.001	relevant diff
FCR	t(45) = -14.8	= 1	t(45) = -16	< 0.001	relevant diff	t(45) = -15.3	= 1	t(45) = -16.8	< 0.001	relevant diff
FCU	t(45) = -3.57	= 1	t(45) = -5.29	< 0.001	relevant diff	t(45) = -3.34	= 0.999	t(45) = -5	< 0.001	relevant diff
PL	t(45) = -8.86	= 1	t(45) = -12.1	< 0.001	relevant diff	t(45) = -10.6	= 1	t(45) = -14.7	< 0.001	relevant diff
FDS 5	t(45) = -1.62	= 0.056	t(45) = 1.899	= 0.064	indeterminate	t(45) = -2.86	= 0.003	t(45) = 2.19	= 0.034	indeterminate
FDS 4	t(45) = -3.74	< 0.001	t(45) = 2.035	= 0.048	equivalent	t(45) = -1.88	= 0.033	t(45) = 2.022	= 0.049	indeterminate
FDS 3	t(45) = -0.764	= 0.224	t(45) = 1.705	= 0.095	indeterminate	t(45) = -1.39	= 0.085	t(45) = 1.179	= 0.245	indeterminate
FDS 2	t(45) = 2.073	= 0.022	t(45) = -1.41	= 0.165	indeterminate	t(45) = 0.783	= 0.219	t(45) = -2.33	= 0.025	indeterminate
FDP 5	t(45) = 0.222	= 0.413	t(45) = -5.72	< 0.001	relevant diff	t(45) = -1.01	= 0.841	t(45) = -8.59	< 0.001	relevant diff
FDP 4	t(45) = 0.083	= 0.533	t(45) = 2.984	= 0.005	indeterminate	t(45) = -2.36	= 0.011	t(45) = 0.244	= 0.808	indeterminate
FDP 2	t(45) = 3.269	= 0.999	t(45) = 5.783	< 0.001	relevant diff	t(45) = -0.93	= 0.179	t(45) = 2.059	= 0.045	indeterminate
FDP 2	t(45) = 1.043	= 0.849	t(45) = 2.926	= 0.005	indeterminate	t(45) = 3.819	< 0.001	t(45) = -1.92	= 0.061	indeterminate
EDC 5	t(45) = 1.554	= 0.936	t(45) = 3.557	< 0.001	relevant diff	t(45) = -0.115	= 0.454	t(45) = 2.316	= 0.025	indeterminate
EDC 4	t(45) = 2.786	= 0.996	t(45) = 4.156	< 0.001	relevant diff	t(45) = 1.132	= 0.868	t(45) = 2.897	= 0.006	indeterminate
EDC 3	t(45) = 1.608	= 0.943	t(45) = 2.71	= 0.009	indeterminate	t(45) = 1.197	= 0.881	t(45) = 2.337	= 0.024	indeterminate
EDC 2	t(45) = 0.897	= 0.813	t(45) = 2.879	= 0.006	indeterminate	t(45) = -2.68	= 0.005	t(45) = 2.871	= 0.006	indeterminate
EDM	t(45) = 2.299	= 0.987	t(45) = 3.956	< 0.001	relevant diff	t(45) = 0.025	= 0.51	t(45) = 2.339	= 0.024	indeterminate
EIP	t(45) = 0.507	= 0.693	t(45) = 2.467	= 0.018	indeterminate	t(45) = -4.5	< 0.001	t(45) = 1.293	= 0.203	equivalent
EPL	t(45) = -2.1	= 0.021	t(45) = 1.091	= 0.281	indeterminate	t(45) = -2.54	= 0.007	t(45) = 0.839	= 0.406	indeterminate
EPB	t(45) = -2.89	= 0.003	t(45) = 0.216	= 0.83	indeterminate	t(45) = 7.628	< 0.001	t(45) = -4.52	< 0.001	trivial diff
FPL	t(45) = -0.54	= 0.704	t(45) = -3.39	= 0.001	indeterminate	t(45) = -1.43	= 0.92	t(45) = -5.74	< 0.001	relevant diff
APL	t(45) = 2.393	= 0.01	t(45) = -0.957	= 0.344	indeterminate	t(45) = 1.993	= 0.026	t(45) = -5.02	< 0.001	relevant diff
APB	t(45) = -0.462	= 0.323	t(45) = 1.952	= 0.057	indeterminate	t(45) = -6.41	< 0.001	t(45) = 0.313	= 0.756	equivalent
FPB	t(45) = -0.182	= 0.428	t(45) = 2.287	= 0.027	indeterminate	t(45) = -8.41	< 0.001	t(45) = 1.113	= 0.272	equivalent

OPP	t(45) = -0.417	= 0.339	t(45) = 2.058	= 0.045	indeterminate	t(45) = -6.72	< 0.001	t(45) = 0.009	= 0.993	equivalent
ADPt	t(45) = 1.139	= 0.13	t(45) = -2.94	= 0.005	indeterminate	t(45) = 3.266	= 0.001	t(45) = -6.94	< 0.001	trivial diff
ADPo	t(45) = 2.622	= 0.006	t(45) = -2.08	= 0.043	indeterminate	t(45) = 6.326	< 0.001	t(45) = -2.95	= 0.005	equivalent
ADM	t(45) = -0.9	= 0.187	t(45) = 2.009	= 0.051	indeterminate	t(45) = -15.9	< 0.001	t(45) = 3.446	= 0.001	trivial diff
FDM	t(45) = -0.765	= 0.224	t(45) = 1.96	= 0.056	indeterminate	t(45) = -12.7	< 0.001	t(45) = 0.497	= 0.622	equivalent

Task	**PG40**					**PG40**				
	EQ		NHST		Interpretation	EQ		NHST		Interpretation
	t-statistic (df)	p-value	t-statistic (df)	p-value		t-statistic (df)	p-value	t-statistic (df)	p-value	
ECRL	t(44) = 8.141	= 1	t(44) = 8.813	< 0.001	relevant diff	t(44) = 5.906	= 1	t(44) = 6.545	< 0.001	relevant diff
ECRB	t(44) = 8.475	= 1	t(44) = 8.965	< 0.001	relevant diff	t(44) = 6.711	= 1	t(44) = 7.34	< 0.001	relevant diff
ECU	t(44) = 4.488	= 1	t(44) = 5.407	< 0.001	relevant diff	t(44) = 3.056	= 0.998	t(44) = 3.713	< 0.001	relevant diff
FCR	t(44) = -17.6	= 1	t(44) = -18.3	< 0.001	relevant diff	t(44) = -19	= 1	t(44) = -19.9	< 0.001	relevant diff
FCU	t(44) = -6.76	= 1	t(44) = -7.69	< 0.001	relevant diff	t(44) = -6.45	= 1	t(44) = -7.34	< 0.001	relevant diff
PL	t(44) = -13.2	= 1	t(44) = -15	< 0.001	relevant diff	t(44) = -12.9	= 1	t(44) = -14.7	< 0.001	relevant diff
FDS5	t(44) = -0.439	= 0.331	t(44) = 1.556	= 0.127	indeterminate	t(44) = -0.204	= 0.42	t(44) = 1.519	= 0.136	indeterminate
FDS4	t(44) = -0.136	= 0.446	t(44) = 2.339	= 0.024	indeterminate	t(44) = 0.014	= 0.505	t(44) = 1.585	= 0.12	indeterminate
FDS3	t(44) = -0.814	= 0.21	t(44) = 1.151	= 0.256	indeterminate	t(44) = 0.96	= 0.171	t(44) = -1.59	= 0.12	indeterminate
FDS2	t(44) = -1.22	= 0.885	t(44) = -2.36	= 0.023	indeterminate	t(44) = -3.29	= 0.999	t(44) = -4.56	< 0.001	relevant diff
FDP5	t(44) = -3.56	= 1	t(44) = -5.65	< 0.001	relevant diff	t(44) = -2.97	= 0.998	t(44) = -4.52	< 0.001	relevant diff
FDP4	t(44) = 0.256	= 0.601	t(44) = 1.636	= 0.109	indeterminate	t(44) = -0.643	= 0.738	t(44) = -1.97	= 0.055	indeterminate
FDP2	t(44) = 4.456	= 1	t(44) = 5.735	< 0.001	relevant diff	t(44) = 0.452	= 0.673	t(44) = 2.233	= 0.031	indeterminate
FDP2	t(44) = 3.177	= 0.999	t(44) = 4.094	< 0.001	relevant diff	t(44) = -1.51	= 0.069	t(44) = 0.507	= 0.614	indeterminate
EDC5	t(44) = 2.878	= 0.997	t(44) = 4.128	< 0.001	relevant diff	t(44) = 0.874	= 0.807	t(44) = 1.72	= 0.093	indeterminate
EDC4	t(44) = 4.237	= 1	t(44) = 5.197	< 0.001	relevant diff	t(44) = 0.923	= 0.819	t(44) = 2.045	= 0.047	indeterminate
EDC3	t(44) = 3.899	= 1	t(44) = 5.551	< 0.001	relevant diff	t(44) = 1.339	= 0.906	t(44) = 2.901	= 0.006	indeterminate
EDC2	t(44) = 2.218	= 0.984	t(44) = 3.933	< 0.001	relevant diff	t(44) = -1.12	= 0.134	t(44) = 0.465	= 0.644	indeterminate
EDM	t(44) = 3.864	= 1	t(44) = 4.92	< 0.001	relevant diff	t(44) = -0.446	= 0.329	t(44) = 1.448	= 0.155	indeterminate
EIP	t(44) = 1.232	= 0.888	t(44) = 2.715	= 0.009	indeterminate	t(44) = 1.114	= 0.136	t(44) = -0.45	= 0.655	indeterminate
EPL	t(44) = -0.306	= 0.38	t(44) = 1.015	= 0.315	indeterminate	t(44) = 0.838	= 0.797	t(44) = 3.473	= 0.001	relevant diff
EPB	t(44) = 0.669	= 0.254	t(44) = -0.868	= 0.39	indeterminate	t(44) = -0.873	= 0.806	t(44) = -3.35	= 0.002	relevant diff
FPL	t(44) = -2.18	= 0.983	t(44) = -3.5	= 0.001	relevant diff	t(44) = -2.3	= 0.987	t(44) = -3.63	< 0.001	relevant diff
APL	t(44) = -0.128	= 0.551	t(44) = -1.51	= 0.139	indeterminate	t(44) = -1	= 0.84	t(44) = -2.75	= 0.009	indeterminate
APB	t(44) = 0.527	= 0.7	t(44) = 1.844	= 0.072	indeterminate	t(44) = -2.2	= 0.017	t(44) = 0.192	= 0.849	indeterminate
FPB	t(44) = 1.055	= 0.851	t(44) = 2.492	= 0.017	indeterminate	t(44) = -3.46	< 0.001	t(44) = 1.175	= 0.246	equivalent
OPP	t(44) = 0.945	= 0.825	t(44) = 2.136	= 0.038	indeterminate	t(44) = -2.3	= 0.013	t(44) = 0.294	= 0.77	indeterminate
ADPt	t(44) = -2.03	= 0.976	t(44) = -4.23	< 0.001	relevant diff	t(44) = -1.59	= 0.941	t(44) = -5.98	< 0.001	relevant diff

ADPo	t(44) = -0.566	= 0.713	t(44) = -3.08	= 0.004	indeterminate	t(44) = 2.332	= 0.012	t(44) = -2.99	= 0.005	indeterminate
ADM	t(44) = 1.188	= 0.879	t(44) = 2.699	= 0.01	indeterminate	t(44) = -3.37	< 0.001	t(44) = 2.513	= 0.016	equivalent
FDM	t(44) = 0.928	= 0.821	t(44) = 2.374	= 0.022	indeterminate	t(44) = -4.86	< 0.001	t(44) = 0.975	= 0.335	equivalent

Task	**Pinch**					**Pinch**				
	EQ		NHST		Interpretation	EQ		NHST		Interpretation
	t-statistic (df)	p-value	t-statistic (df)	p-value		t-statistic (df)	p-value	t-statistic (df)	p-value	
ECRL	t(33) = 0.847	= 0.202	t(33) = -1.02	= 0.314	indeterminate	t(33) = 2.384	= 0.988	t(33) = 3.816	< 0.001	relevant diff
ECRB	t(33) = 0.752	= 0.229	t(33) = -0.442	= 0.661	indeterminate	t(33) = -0.445	= 0.329	t(33) = 0.831	= 0.412	indeterminate
ECU	t(33) = 0.316	= 0.377	t(33) = -0.904	= 0.373	indeterminate	t(33) = 1.368	= 0.09	t(33) = -1.19	= 0.242	indeterminate
FCR	t(33) = 0.348	= 0.365	t(33) = -0.869	= 0.391	indeterminate	t(33) = -2.19	= 0.018	t(33) = 0.156	= 0.877	indeterminate
FCU	t(33) = -0.109	= 0.543	t(33) = -2	= 0.054	indeterminate	t(33) = -0.0117	= 0.505	t(33) = -2.59	= 0.014	indeterminate
PL	t(33) = -0.168	= 0.566	t(33) = -1.14	= 0.262	indeterminate	t(33) = 0.795	= 0.216	t(33) = -1.03	= 0.309	indeterminate
FDS5	t(33) = -0.913	= 0.816	t(33) = -1.22	= 0.231	indeterminate	t(33) = -5.66	= 1	t(33) = -6.37	< 0.001	relevant diff
FDS4	t(33) = -0.903	= 0.813	t(33) = -1.34	= 0.19	indeterminate	t(33) = -0.287	= 0.612	t(33) = -2.45	= 0.02	relevant diff
FDS3	t(33) = -1.09	= 0.141	t(33) = 0.525	= 0.603	indeterminate	t(33) = -1.49	= 0.927	t(33) = -4.23	< 0.001	relevant diff
FDS2	t(33) = 0.77	= 0.223	t(33) = -0.073	= 0.942	indeterminate	t(33) = -1.66	= 0.947	t(33) = -2.71	= 0.011	relevant diff
FDP5	t(33) = -2.14	= 0.98	t(33) = -3.96	< 0.001	relevant diff	t(33) = -7.97	= 1	t(33) = -9.85	< 0.001	relevant diff
FDP4	t(33) = -3.03	= 0.998	t(33) = -4.24	< 0.001	relevant diff	t(33) = -7.42	= 1	t(33) = -8.87	< 0.001	relevant diff
FDP2	t(33) = 0.836	= 0.204	t(33) = -0.65	= 0.52	indeterminate	t(33) = -8.11	= 1	t(33) = -11.3	< 0.001	relevant diff
FDP2	t(33) = 0.052	= 0.521	t(33) = 1.171	= 0.25	indeterminate	t(33) = -5.24	= 1	t(33) = -6.91	< 0.001	relevant diff
EDC5	t(33) = 1.103	= 0.139	t(33) = -1.54	= 0.134	indeterminate	t(33) = 2.548	= 0.008	t(33) = -0.386	= 0.702	indeterminate
EDC4	t(33) = 1.556	= 0.065	t(33) = -1.12	= 0.27	indeterminate	t(33) = -2.43	= 0.01	t(33) = 0.021	= 0.984	indeterminate
EDC3	t(33) = -0.135	= 0.553	t(33) = -1.06	= 0.299	indeterminate	t(33) = 0.498	= 0.311	t(33) = -0.958	= 0.345	indeterminate
EDC2	t(33) = -0.288	= 0.612	t(33) = -1.13	= 0.265	indeterminate	t(33) = 0.911	= 0.184	t(33) = -0.457	= 0.651	indeterminate
EDM	t(33) = -1.05	= 0.849	t(33) = -2.1	= 0.044	indeterminate	t(33) = 1.093	= 0.141	t(33) = -0.561	= 0.579	indeterminate
EIP	t(33) = -0.494	= 0.688	t(33) = -1.31	= 0.198	indeterminate	t(33) = 0.833	= 0.206	t(33) = -0.552	= 0.585	indeterminate
EPL	t(33) = -2.36	= 0.012	t(33) = 0.192	= 0.849	indeterminate	t(33) = -4.09	< 0.001	t(33) = 1.947	= 0.06	equivalent
EPB	t(33) = 1.296	= 0.102	t(33) = -0.255	= 0.8	indeterminate	t(33) = -7.17	< 0.001	t(33) = 0.922	= 0.363	equivalent
FPL	t(33) = -0.2	= 0.578	t(33) = -1.8	= 0.081	indeterminate	t(33) = -1.83	= 0.962	t(33) = -4.07	< 0.001	relevant diff
APL	t(33) = -1.1	= 0.861	t(33) = -2.03	= 0.051	indeterminate	t(33) = -3.11	= 0.998	t(33) = -4.49	< 0.001	relevant diff
APB	t(33) = -2.11	= 0.979	t(33) = -2.73	= 0.01	indeterminate	t(33) = -2.37	= 0.988	t(33) = -3.05	= 0.005	indeterminate
FPB	t(33) = -0.816	= 0.79	t(33) = -1.71	= 0.096	indeterminate	t(33) = -1.29	= 0.898	t(33) = -4.24	< 0.001	relevant diff
OPP	t(33) = -5.13	= 1	t(33) = -5.74	< 0.001	relevant diff	t(33) = -6.93	= 1	t(33) = -7.68	< 0.001	relevant diff
ADPt	t(33) = -1.78	= 0.042	t(33) = 0.96	= 0.344	indeterminate	t(33) = -1.84	= 0.038	t(33) = 2.612	= 0.013	indeterminate
ADPo	t(33) = -2.19	= 0.018	t(33) = 1.33	= 0.193	indeterminate	t(33) = -1.68	= 0.051	t(33) = 3.116	= 0.004	indeterminate
ADM	t(33) = -0.757	= 0.773	t(33) = -1.62	= 0.114	indeterminate	t(33) = -1.26	= 0.891	t(33) = -2.79	= 0.009	indeterminate

FDM	t(33) = -0.502	= 0.69	t(33) = -1.37	= 0.179	indeterminate	t(33) = -0.649	= 0.74	t(33) = -2.2	= 0.035	indeterminate

APPENDIX C –ETHICS CONSENT FORM

Letter of Information and Consent

Quantification of Load Distribution on the Hands and Fingers

Faculty Supervisor:
Peter Keir, PhD
Professor
Department of Kinesiology
McMaster University
(905) 525-9140 ext. 23543

Student Investigator
Ryan Chhiba, MSc Candidate
Department of Kinesiology
McMaster University
(416) 624-2310

Paul Tilley,
Undergraduate Thesis Student
Department of Kinesiology
McMaster University
416-998-5640

Purpose of the Study
The hand is our primary tool for performing mechanical interactions with the external environment. Due to its complex anatomy and frequency of use, the hand is exposed to limitless combinations of mechanical demands, many of which are identified as risk factors for musculoskeletal disorders. Biomechanical models are used to determine the internal joint moments, and muscle forces of the hand under external loading. However, individual differences limit the generalizability and clinical utility of hand models. Thus, the purpose of this study will be to assess the sensitivity of biomechanical hand model estimated joint moments and muscle forces under external loading to variation in hand segment parameters, joint angles, and load distribution. This study will clarify the role of load placement and load distribution on internal joint moments and muscle forces in the hand, facilitating the development of hand models which are more representative of how the hand is loaded during occupational tasks and everyday activities.

Procedures involved in the Research
This study will involve a single laboratory session taking approximately 1 hour to complete. All procedures will be completed by the researchers in the study.

1) Before the participant enters the Laboratory, they will have successfully completed their COVID-19 Self-Screening and show their MacCheck to Mr. Tilley or Mr. Chhiba upon entering. The participant will be asked to sanitize their hands with the provided hand sanitizer.

2) An informed consent form with details of the experiment will be explained and all questions will be answered before signing.

3) To minimize close contact, one of three gloves containing pre-placed sensors will be chosen by the participant based on best fit. The participant will then be instructed to put the glove on their right hand and will be showed how to secure the device on their forearm through mimicked actions from one of the investigators.

4) Participants will be seated at the assessment table, and muscles to be measured with EMG will be palpated by one of the researchers. Participants will be asked to flex certain joints to ensure the location of the specific muscles being tested. Electrodes will be affixed to the skin over the right forearm to record muscle activity for the forearm and finger flexors. The electrodes will be taped down using tape. These areas will be shaved with a new, disposable razor and cleaned off with alcohol prior to the application of the electrodes. These procedures are required to obtain a high quality signal.

5) Markers will be placed on the participants by one of the researchers to collect motion capture data. Anatomical landmarks will be palpated and participants will be asked to flex certain joints to ensure the location of the specific body being collected. Markers will be placed at landmarks on the right shoulder, elbow, wrist, palm, middle finger and thumb. The marker will be taped down using tape. These procedures are required to obtain a high quality signal.

6) Once the collection devices are secure, the participant will be asked to make their way to the platform and stand in the designated area. Participants will be asked to complete a series of maximum voluntary grips. The grips are:

i) A static, full hand grasp of a hand grip dynamometer.

Each maximum voluntary grip will be held for 10 seconds and repeated 3 times. Two minuted of rest will be given between repetitions.

7) Participants will then be asked to complete a series of static common gripping tasks at specific levels of their maximum voluntary grips. The tasks are:

i, ii) A static, full hand grasp of a hand grip dynamometer at 20%, 40%, of their maximum voluntary power grip force
iii) A static, pinch grasp of a force transducer at 50 N
iv, v, vi, vii) A static single finger press on a force transducer at 10 N (finger fully extended) (completed for each finger, index, middle, ring and pinky)
viii) A two-finger press on a force transducer at 15 N (index and middle finger fully extended)
ix) A three finger press on a force transducer at 20 N (index, middle, and ring finger fully extended)
x) A four finger press on a force transducer at 25 N (index, middle, ring, and pinky finger fully extended)
xi) A dynamic index finger pressing task at 10 N (finger fully extended)

Each task will be held for 10 seconds and repeated 3 times. At the direction of the investigator, the participant will hold the force transducer/ dynamometer from the table, ramp up to the specified force and then maintain it for 10 seconds, and return it to the table. All grasping tasks will be performed standing with at 90 degrees of elbow flexion.
8) The participant will remove the glove at the direction of the investigators and leave them on the table in front of them.

Potential Harms, Risks or Discomforts
Minimal risks are anticipated from this study.

Muscle Fatigue
You may feel fatigued following the session due to the repetitive grasping motions. You will be given 2 minutes rest between grasps to mitigate these effects but may still experience fatigue similar to that following a light workout.

Injury

a) If the participant drops one of the items being held, there is a risk of the glass breaking or a blunt force (very minimal as objects are light weight) to the foot.
b) all tasks are completed over a table so if the object falls, it will fall onto the table instead of the participant. Participants will not be allowed to enter the lab space without proper footwear to protect their feet

Skin Sensitivity
You may experience mild skin irritation/redness from the adhesive of the electrodes. This is similar to the irritation that may be caused by a bandage and typically fades within 2 to 3 days.

COVID-19 Risks
In light of the current global COVID-19 pandemic, Canadian public health authorities have strongly recommended that everyone takes additional precautions, including those outlined in this letter. McMaster University is attempting to limit the risk of exposure to COVID-19 by using reasonable efforts to follow the health and safety guidelines recommended by the provincial and federal health authorities. Nevertheless, there remains a risk that by attending McMaster University campus or any of the McMaster University Study sites, you may contract COVID-19. COVID-19 can result in severe illness, medical expenses, loss of income and death. The university has taken every reasonable precaution and implemented guidance documents and COVID-19 precautions in our buildings for our community

Potential Benefits
The outcome of the study will allow us to inform occupational guidelines. The research will not benefit you directly.

Confidentiality:
Your identity will be kept confidential, and data collected will be used for research purposes only. The information directly pertaining to you will be locked in a cabinet or stored electronically on a password protected computer for 10 years. Unidentifiable data will be shared to an open source modelling platform OpenSim database for other researcher to use in order to improve their models. During the collection there may be undergraduate research assistants present in the lab space.

Participation:
Your participation in this study is voluntary. If you decide to participate, you can decide to stop at any time, even after signing the consent form or part-way through the study. If you decide to stop participating, there will be no consequences to you. If you chose to withdraw at any time in the study, you will still be compensated for your time. Once the data collection is completed, you will not be able to withdraw form the study as the data will remain anonymous.

Incentive
You will receive $20 cash for participating in this study as remuneration for your time. Your contact information may be shared with the Kin Grad Admin to ensure your compensation. The amount received is taxable. It is your responsibility to report this amount for income tax purposes

Information about the Study Results:
You may obtain information about the study results by contacting Dr. Peter Keir at (905) 525-9140 (x 23543) or indicating “Yes” at the bottom of this form.

Questions about the Study:
If you have questions or need more information about the study itself, please contact me at:

Ryan Chhiba
chhibar@mcmaster.ca

This study has been reviewed by the McMaster University Research Ethics Board and received ethics clearance. If you have concerns or questions about your rights as a participant or about the way the study is conducted, please contact: McMaster Research Ethics Secretariat, c/o Research Office for Administrative Development and Support, E-mail: ethicsoffice@mcmaster.ca, Phone: (905) 525-9140 ext. 23142

CONSENT

- I have read the information presented in the information letter about a study being conducted by, Mr. Ryan Chhiba, Mr. Paul Tilley and Dr. Peter Keir of McMaster University
- I have had the opportunity to ask questions about my involvement in this study and to receive additional details I requested
- I understand that if I agree to participate in this study, I may withdraw from the study at any time. If I choose to withdraw from the study after the collection, my data will still be used for analysis.
- I understand I will receive a signed copy of this form via email
- I agree to participate in the study
- I agree to having part of my upper extremities (Shoulder, arm, hand, torso) recorded via infrared motion capture to collect motion capture data
- I understand that upon publication, non-identifiable data collected in this study might be shared to open source modelling databases for an indefinite amount of time.

Signature: _____ Date: _____

Name of Participant (Printed) _____

1. ___Yes, I would like to receive a summary of the study's results
Please send them to me at this email address _____
Or to this mailing address: _____
_____
_____

___ No, I do not want to receive a summary of the study's results

I have received my $20 incentive in cash

Signature: _____ Date: _____

Name of Participant (Printed) _____

MAC ID & Student Number (if applicable) _____

Email : _____

Person Obtaining Consent

Signature: _____ Date: _____

Name of Researcher (Printed) _____